AD-A034 945 AIR FORCE INST OF TECH WRIGHT-PATTERSON AFB OHIO SCH--ETC F/G 22/2
A FUEL CONSERVATION NEAR-OPTIMAL CONTROL LAW FOR AN EVADING SPA--ETC(U)
DEC 76 W V GREEN
UNCLASSIFIED GA/MC/76D-8 NL

| OF |
AD
A034945

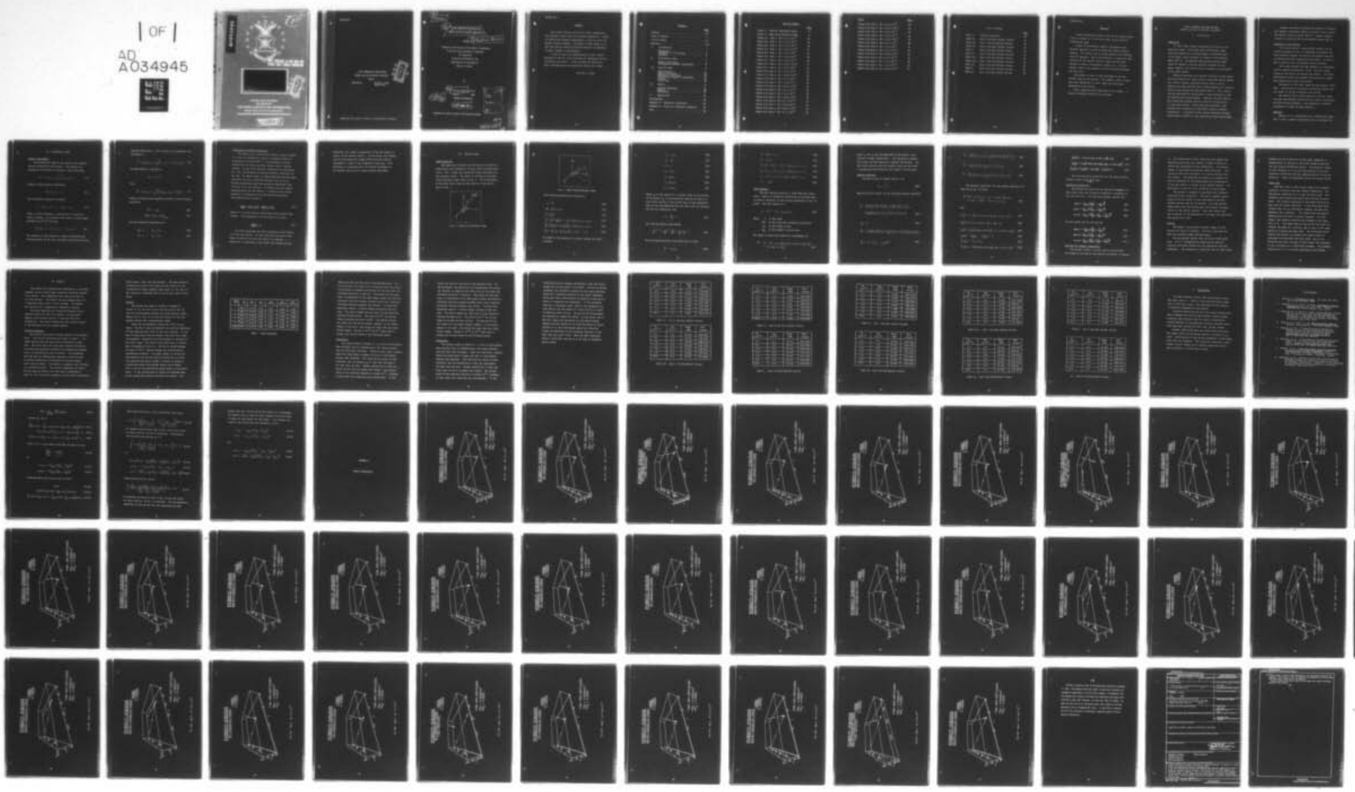

END
DATE
FILMED
3-77

UNITED STATES AIR FORCE

AIR UNIVERSITY

AIR FORCE INSTITUTE OF TECHNOLOGY

Wright-Patterson Air Force Base, Ohio

GA/MC/76D-8

A FUEL CONSERVATION NEAR-OPTIMAL CONTROL LAW FOR AN EVADING SPACECRAFT

THESIS

GA/MC/76D-8

William V. Green
Captain USAF

Approved for public release; distribution unlimited

GA/MC/76D-8

A FUEL CONSERVATION NEAR-OPTIMAL CONTROL LAW FOR AN EVADING SPACECRAFT

THESIS Master's thesis,

Presented to the Faculty of the School of Engineering

of the Air Force Institute of Technology

Air University

in Partial Fulfillment of the

Requirements for the Degree of

Master of Science

by

William V. Green B.S.A.E.

Captain USAF

Graduate Astronautics

Dec[redacted]76

Approved for public release; distribution unlimited

Preface

This report studies the use of a fuel conservation near-optimal control law by an evading spacecraft. A form of differential dynamic programming is used to solve the optimal control problem. The object of this study is to test the control against different pursuers to determine if such a scheme is advantageous.

I wish to express my appreciation to Prof. Gerald Anderson of the Air Force Institute of Technology for his assistance and advice. I wish to thank my family for their consideration and cooperation during this study.

William V. Green

Contents

List of Figures

List of Tables

Abstract

A fuel conservation control law for an evading spacecraft is tested in a free final time, pursuit-evasion differential game.

A form of differential dynamic programming with periodic updating is used to solve the optimal control problem. The control law is tested against two different kinds of pursuers. One of the pursuers is using the same updating of the optimal control scheme and the other pursuer is using a non-optimal control law. The non-optimal control law produces a collision course between the two craft.

The evader is able to take advantage of any non-optimal play by the pursuer. The evader is able to optimize the combination of final range and final mass, depending on the mission.

Plots comparing the flight path of the evader and several different pursuers are included.

A FUEL CONSERVATION NEAR OPTIMAL CONTROL LAW FOR AN EVADING SPACECRAFT

I. Introduction

Background

In 1954, Rufus Isaacs introduced the theory of differential games. Since that time, differential games have been applied to a diverse number of problem areas. In his book, Isaacs develops the theory of differential games (Ref 1). He examines some pursuit-evasion games using his theory to provide minimax solutions to the games. However, the pursuit-evasion examples are developed using simple models.

Anderson developed near-optimal solutions to non-linear, zero-sum differential games using a transition matrix method and a matrix Racatti backsweep method (Refs 5 and 6). Anderson and Bohn applied both of these methods to a pursuit-evasion game between two spacecraft (Ref 3). This control law was developed for the pursuer to take advantage of the non-optimal play of the evader. Anderson and Bohn applied the closed-loop control law to a realistic problem with a large state vector. There were some problems in the methods with instability of the matrix Racatti backward integration. A solution to the initial two-point boundary value problem (TPBVP) is also required to start the methods.

Jacobson and Mayne developed the method of Differential Dynamic Programming (DDP) to provide a way to solve the optimal control problem (Ref 2). Jarmark suggest a method of applying DDP to differential games (Ref 7).

Statement of the Problem

This study applies a near-optimal control for an evading spacecraft which is attempting to maximize the final distance between the pursuer and himself and also to minimize the fuel required by the evader. A form of DDP is used to solve the optimal control problem.

This study assumes two-body dynamics in a Newtonian, inverse square gravitational field. The only forces acting on the bodies are gravity and thrust. All other perturbative forces are assumed insignificant in magnitude compared to thrust and gravity.

The payoff is the final range and the evader's final mass. The pursuer is trying to minimize the payoff and the evader is trying to maximize the payoff.

The control law is tested against a pursuer using the same near-optimal control and one using a non-optimal collision course guidance. The assumption of perfect information is made for both pursuers.

Approach

Chpater II is a description of a differential game. This is only a general description and is not meant as a detailed reference. The development is along the lines of Bryson and Ho (Ref 4). Also in Chapter II is a brief overview of the DDP method used in this study. Chapter III is the specific game that is addressed in this study. This chapter contains the specific equations and assumptions used to formulate the control law. Chapter IV contains the results of applying the control law. A discussion of the results is also contained. The conclusions are contained in Chapter V.

II. Differential Game

<u>General Development</u>

The differential game is the result of an optimal control problem with two players. The players are attempting to minimize or maximize a cost functional

$$J = \phi[x(t_f), t_f] + \int_{t_o}^{t_f} L(x,u,v,t)\, dt \qquad (1)$$

Subject to the terminal constraints

$$\psi(x(t_f), t_f) = 0 \qquad (2)$$

and the dynamic equations of motion

$$\dot{x} = f(x,u,v,t) \quad ; \quad x(t_o) = x_o \qquad (3)$$

where u is the minimizer's control and v is the maximizer's control. The controls that result in the minimax solution are u^0, v^0 such that

$$J(u^o, v) \le J(u^o, v^o) \le J(u, v^o) \qquad (4)$$

The solution to this problem is found by adjoining the state equations to the cost functional using time varying

Lagrange multipliers. This results in an augmented cost functional $\tilde{J}$

$$\tilde{J} = \phi(x(t_f), t_f) + \int_{t_0}^{t_f} \left[L(x, u, v, t) + \lambda^T (f - \dot{x}) \right] dt \tag{5}$$

The Hamiltonian is defined as

$$H = L + \lambda^T f \tag{6}$$

thus

$$\tilde{J} = \phi(x(t_f), t_f) + \int_{t_0}^{t_f} \left[H(x, u, v, \lambda, t) - \lambda^T \dot{x} \right] dt \tag{7}$$

Taking a variation and expanding results in the following conditions

$$\dot{\lambda}^T = -H_x \tag{8}$$

$$\lambda(t_f) = \left(\phi_x + \nu^T \psi_x \right) \Big|_{t=t_f} \tag{9}$$

and the optimality conditions are

$$H_u = 0 \quad ; \quad H_{uu} \geq 0 \tag{10}$$

$$H_v = 0 \quad ; \quad H_{vv} \leq 0 \tag{11}$$

Differential Dynamic Programming

The method used to solve this optimal control problem is a form of differential dynamic programming (DDP) as suggested by Jarmark (Ref 7). The procedure involves integrating the state equations forward with a guessed control. At the final time the transversality conditions, Eq. (10), are enforced to provide boundary conditions for Eq. (9). As shown in Ref. 8, these equations and the state equations are then integrated backward from t_f to t_0. At each integration step the optimality conditions, Eqs. (10) and (11), are enforced. To predict the cost change caused by using the new control, a predicted cost change equation is integrated along the backward trajectory. The predicted cost change is

$$\dot{a}(t) = H(x, u, \lambda, t) - H(x, \bar{u}, \lambda, t) \tag{12}$$

where $\bar{u}$ is the new control found during the backward integration. This equations is initialized at t_f using

$$a(t_f) = 0 \tag{13}$$

The state equations are then integrated forward again, using the new control. At the final time the actual cost change resulting from the new control is computed. A comparison is then made of the actual cost change and the predicted cost change to determine if the new control is closer to the optimal control. If the actual cost change and the predicted cost change differ too much then an adjustment is made in the integration step size. This procedure is continued until the control converges to the optimal and the cost change becomes negligible.

III. Specific Game

State Equations

The equations of motion are derived using spherical coordinates and a Newtonian, inverse square gravitational field. Fig. 1 shows the coordinate frame used where R is the position vector. The thrust is defined in the body fixed reference frame shown in Fig. 2. The relationship of the body fixed frame and the inertial frame can be seen in Fig. 1.

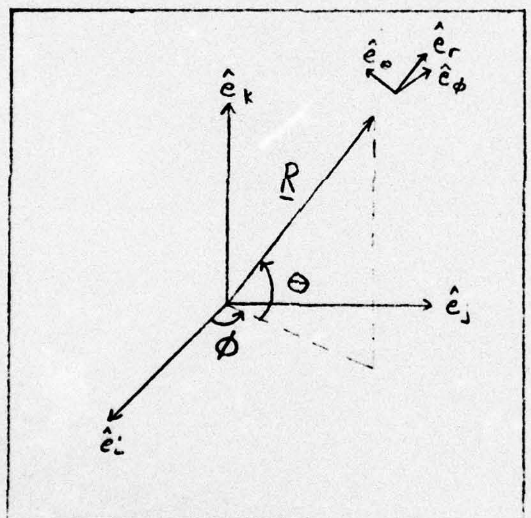

Fig. 1 Inertial Coordinate Frame

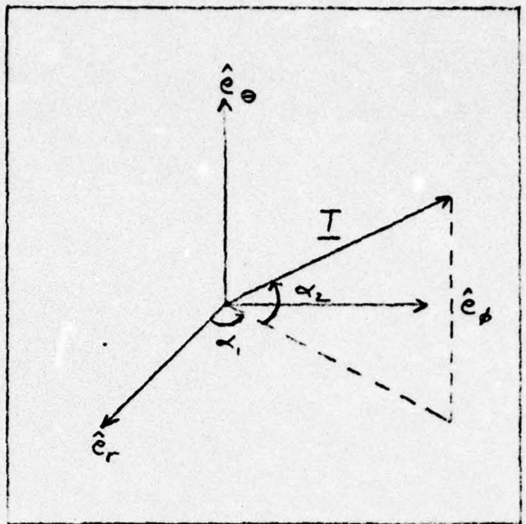

Fig. 2 Body Fixed Reference Frame

The resulting equations of motion are

$$\dot{r} = V_r \tag{14}$$

$$\dot{\phi} = V_\phi / r \cos\theta \tag{15}$$

$$\dot{\theta} = V_\theta / r \tag{16}$$

$$\dot{V}_r = (V_\phi^2 + V_\theta^2)/r - \mu/r^2 + (T/m)\cos\alpha_2 \cos\alpha_1 \tag{17}$$

$$\dot{V}_\phi = (V_\phi V_\theta \tan\theta - V_\phi V_r)/r + (T/m)\cos\alpha_2 \sin\alpha_1 \tag{18}$$

$$\dot{V}_\theta = -(V_r V_\theta + V_\phi^2 \tan\theta)/r + (T/m)\sin\alpha_2 \tag{19}$$

To normalize the equations of motion, define the state variables

$$x_1 = r/r_0 \tag{20}$$

$$x_2 = \phi \tag{21}$$

$$x_3 = \theta \tag{22}$$

$$x_4 = V_r/V_0 \tag{23}$$

$$x_5 = V_\phi/V_0 \tag{24}$$

$$x_6 = V_\theta/V_0 \tag{25}$$

$$x_7 = m/m_0 \tag{26}$$

where r_0 is the radius of a circular orbit at the surface of the earth, V_0 is the transverse velocity of that circular orbit and M_0 is the initial mass of the spacecraft. Next we can non-dimensionalize the time units by introducing the non-dimensional unit

$$\tau = \frac{V_0}{r_0} t \tag{27}$$

The time derivatives then become

$$\frac{d}{d\tau}(\,) = \frac{d(\,)}{dt}\frac{dt}{d\tau} = \frac{r_0}{V_0}\frac{d}{d\tau}(\,) \tag{28}$$

The non-dimensionalized state equations are then

$$\dot{x}_1 = x_4/x_1 \tag{29}$$

$$\dot{x}_2 = x_5/(x_1 \cos x_3) \tag{30}$$

$$\dot{x}_3 = x_6/x_1 \tag{31}$$

$$\dot{x}_4 = (x_5^2 + x_6^2)/x_1 - 1/x_1^2 + (T/x_7)\cos\alpha_2 \cos\alpha_1 \tag{32}$$

$$\dot{x}_5 = (x_5 x_6 + x_5^2 \tan x_3)/x_1 + (T/x_7)\cos\alpha_2 \sin\alpha_1 \tag{33}$$

$$\dot{x}_6 = -(x_4 x_6 + x_5^2 \tan x_3)/x_1 + (T/x_7)\sin\alpha_2 \tag{34}$$

$$\dot{x}_7 = -T/c \tag{35}$$

Cost Function

The cost function contains a range term and a mass term. There is a weighting coefficient on the mass term to allow a variation in the relative magnitude of the two terms. The cost function is

$$J = \frac{1}{2} R^2 + F_{mc}(m_e/m_{eo}) \tag{36}$$

where
- R is the range
- Fmc is the final mass weighting coefficient
- m_e is the evader's mass
- m_{eo} is the evader's initial mass

The range is found using spherical trigonometry as

$$R^2 = r_e^2 + r_p^2 - 2 r_e r_p [\cos\theta_e \cos\theta_p \cos(\phi_e - \phi_p) + \sin\theta_e \sin\theta_p] \tag{37}$$

where r_e and r_p are the magnitude of the evader's and pursuer's ranges respectively. The subscript e denotes the evader and the subscript p denotes the pursuer. The mass term contains only the evader's mass and this term is normalized by dividing by the evader's initial mass.

Adjoint Equations

The Hamiltonian is formed from Eq. (7)

$$H = \lambda^T f \tag{38}$$

Applying Eq.(9) results in the following adjoint equations

$$\dot{\lambda}_r = \frac{\lambda_\phi V_\phi / \cos\theta + \lambda_\theta V_\theta + \lambda_{V_r}\left(V_\theta^2 + V_\phi^2\right) - 2\lambda_{V_r}}{r}$$

$$+ \frac{\lambda_{V_\phi} V_\phi \left(V_\theta \tan\theta - V_r\right) - \lambda_{V_\theta}\left(V_r V_\theta + V_\phi^2 \tan\theta\right)}{r} \tag{39}$$

$$\dot{\lambda}_\phi = 0 \tag{40}$$

$$\dot{\lambda}_\theta = \frac{-\lambda_\phi V_\phi \sin\theta / \cos^2\theta - \lambda_{V_\phi} V_\phi V_\theta \sec^2\theta + \lambda_{V_\theta} V_\phi^2 \sec^2\theta}{r} \tag{41}$$

$$\dot{\lambda}_{V_r} = -\lambda_r + \left(\lambda_{V_\phi} + \lambda_{V_\theta} V_\theta\right)/r \tag{42}$$

$$\dot{\lambda}_{V_\phi} = \frac{-\lambda_\phi/\cos\theta - 2\lambda_{V_r} V_\phi - \lambda_{V_\phi} V_\theta \tan\theta - 2\lambda_{V_\theta} V_\phi \tan\theta}{r} \qquad (43)$$

$$\dot{\lambda}_{V_\theta} = \frac{-\lambda_\theta - 2\lambda_{V_r} V_\theta - \lambda_{V_\phi} V_\phi \tan\theta + \lambda_{V_\theta} V_r}{r} \qquad (44)$$

$$\dot{\lambda}_m = \frac{T[(\lambda_{V_r}\cos\alpha_1 + \lambda_{V_\phi}\sin\alpha_1)\cos\alpha_2 + \lambda_{V_\theta}\sin\alpha_2]}{m^2} \qquad (45)$$

The boundary conditions for the adjoint equations are found using eq. (9) where

$$\phi = \tfrac{1}{2}[r_e^2 + r_p^2 - 2r_e r_p(\cos\theta_e \cos\theta_p \cos(\phi_e - \phi_p) + \sin\theta_e \sin\theta_p)] + Fmc\,(m_e/m_{eo}) \qquad (46)$$

thus

$$\lambda_{r_e}(t_f) = r_e - r_p[\cos\theta_e \cos\theta_p \cos(\phi_e - \phi_p) + \sin\theta_e \sin\theta_p] \qquad (47)$$

$$\lambda_{\phi_e}(t_f) = r_e r_p \cos\theta_e \cos\theta_p \sin(\phi_e - \phi_p) \qquad (48)$$

$$\lambda_{\theta_e}(t_f) = r_e r_p[\sin\theta_e \cos\theta_p \cos(\phi_e - \phi_p) - \sin\theta_p \cos\theta_e] \qquad (49)$$

$$\lambda_{V_{r_e}}(t_f) = \lambda_{V_{\phi_e}}(t_f) = \lambda_{V_{\theta_e}}(t_f) = 0 \qquad (50)$$

$$\lambda_{m_e}(t_f) = Fmc/m_{eo} \qquad (51)$$

$$\lambda_{r_p}(t_f) = r_p - r_e[\cos\theta_e \cos\theta_p \cos(\phi_e - \phi_p) + \sin\theta_e \sin\theta_p] \qquad (52)$$

$$\lambda_{\phi p}(t_f) = -r_e r_p \cos\theta_e \cos\theta_p \sin(\phi_e - \phi_p) \qquad (53)$$

$$\lambda_{\theta p}(t_f) = r_e r_p[\cos\theta_e \sin\theta_p \cos(\phi_e - \phi_p) - \sin\theta_e \cos\theta_p] \qquad (54)$$

$$\lambda_{r_p}(t_f) = \lambda_{v_\phi p}(t_f) = \lambda_{v_\theta p}(t_f) = \lambda_{mp}(t_f) = 0 \qquad (55)$$

The transversality conditions are the same for both players except for λ_r, λ_ϕ and λ_m.

Optimality Conditions

The optimality conditions are derived in Appendix A. They result when the inequality condition is enforced in Eqs. (10) and (11). The resulting optimal controls are

$$\sin\alpha_1 = \lambda_{v_\phi e} / (\lambda^2_{v_r e} + \lambda^2_{v_\phi e})^{1/2} \qquad (56)$$

$$\cos\alpha_1 = \lambda_{v_r e} / (\lambda^2_{v_r e} + \lambda^2_{v_\phi e})^{1/2} \qquad (57)$$

$$\sin\alpha_2 = \lambda_{v_\theta e} / (\lambda^2_{v_r e} + \lambda^2_{v_\phi e} + \lambda^2_{v_\theta e})^{1/2} \qquad (58)$$

for the evader and for the pursuer

$$\sin\alpha_1 = -\lambda_{v_\phi p} / (\lambda^2_{v_r p} + \lambda^2_{v_\phi p})^{1/2} \qquad (59)$$

$$\cos\alpha_1 = -\lambda_{v_r p} / (\lambda^2_{v_r p} + \lambda^2_{v_\phi p})^{1/2} \qquad (60)$$

$$\sin\alpha_2 = -\lambda_{v_\theta p} / (\lambda^2_{v_r p} + \lambda^2_{v_\phi p} + \lambda^2_{v_\theta p})^{1/2} \qquad (61)$$

Differential Dynamic Programming

The optimal control is found using a from of DDP. The scheme is the same as the general discussion in Chapter

II. The method used in this study does not compare the predicted and actual cost change in order to adjust or modify the convergence of the integration. The control change is constrained to prevent large variations. This restricts the state trajectory to a weak variation from the nominal. The predicted and actual cost changes are used to determine if the method should be converging or if the new control is closer to the optimal control. The DDP method is used for five iterations at each update.

The control is updated at specified time intervals along the flight trajectory. The new or updated control should allow the evader to take advantage of any non-optimal control used by the pursuer. By using the DDP method many times during the game, the control converges slowly to the optimal control. Thus, the control may not be optimal at the beginning of the game, but approaches the optimal with time.

Pursuer

The evader's near-optimal control scheme is used against two types of pursuers. The first type uses the same near-optimal scheme outlined above.

The non-optimal pursuer uses collision course guidance. This is implemented by resolving the inertial velocity difference between the two spacecraft into two components. One component is along the line of sight (LOS) between the two spacecraft and the other component is perpendicular to the LOS in the plane formed by the LOS and the velocity difference vector. The pursuer's thrust is then directed so as to null the velocity in the perpendicular direction with any remaining thrust in the LOS direction. These two components define the thrust vector.

Final Time

The final time is free in this study and a stopping condition is used to stop the forward integration. The theoretical condition of $\dot{J} = 0$ was initially used. This condition was solved analytically and involved the mass terms. The relative magnitude of the range term and the mass term are rather important. If the final mass coefficient (Fmc) is not judiciously choosen, the mass term dominates the $\dot{J}$ equation. This could force the game to continue past the time of closest approach. For this reason, the stopping condition was changed to the range rate, or $\dot{R}$. This means that as long as the two craft are closing, the game will continue, but as soon as the range begins to increase the game stops. Any strategies which require the pursuer to increase the range to gain an advantage are precluded from this study. Due to the distances and times involved in this study, this strategy is not considered as a significant strategy. The stopping condition of $\dot{R} = 0$ is solved analytically and checked after each integration step. By using the $\dot{R}$ condition, the Fmc can be adjusted to meet the requirements of the evader's mission and not the game stopping condition. If the evader were critically short on fuel, then he could increase the Fmc to gain a fuel savings and still maintain an acceptable miss distance.

IV. Results

The control law algorithm was simulated on a CDC 6600 computer using a fourth order predictor-corrector integration routine. The integration step size was 0.005 TU, or 4.034 seconds. The control law was updated every six integration steps, which is 24.2 seconds. The method was started with a Runga-Kutta integration routine.

The state equations are integrated forward using a quessed control for the first update. On successive updates, the previous control is used for the first integration. The initial update uses the velocity vector as the direction for the guessed control.

Initial Conditions

The control algorithm is tested against five different cases. The initial conditions are shown in Table I. The evader begins from the same initial conditions in each case. The first four test cases were choosen arbitrarily by taking the equations of motion and integrating backward from a collocated point with no thrust. The assumption was made that an intercepting spacecraft would not have to thrust excessively to intercept an orbiting spacecraft with no thrust. The evader is assumed to be initially in a stabilized orbit. The initial conditions for case V are the same as those of the last case in Reference 3. Cases II, III, and IV are coplanar in the initial conditions, while cases I and V are non-coplanar. The same equations of motion are used in all cases and the control is not restricted to planar changes, thus cases II, III, and IV may involve an intercept that is out of the initial orbit plane.

Results

The results are shown in Tables II through XI. Tables II, IV, VI, VIII, and X are the results for the case of a near-optimal pursuer and a near-optimal evader. Tables III, V, VII, IX, XI are the results for the non-optimal pursuer and a near-optimal evader.

There are two parameters which are varied in the study. The Fmc is used to determine the relative magnitude of the range and mass terms in the cost function. If the mass is given more relative weight, then the final range is decreased. Decreasing the Fmc produces an increase in the final range. The ratio of the final mass to initial mass is between 0.7 and 1.0. The Fmc is varied between 0.0 and 4×10^{-3}. Control changes are constrained by preselected constants. The angle change is arbitrarily restricted to 10° and the thrust restriction is varied. The unconstrained thrust change is either no change or a bang-bang change from maximum thrust to no thrust. This is due to the Hamiltonian being linear in the thrust terms. If the coefficients of thrust are combined they can be termed the switching function for thrust. The

Case (No.)	R (KM)	Ø (DEG.)	θ (DEG.)	Vr (KM/SEC)	VØ (DEG/SEC)	Vθ (DEG/SEC)
1	6524.9	70.473	3.953	0.545	-0.025	-0.027
2	6505.7	70.531	0.000	0.478	-0.025	0.000
3	6467.5	70.302	0.000	0.510	-0.023	0.000
4	6467.5	63.541	0.000	0.510	0.023	0.000
5	6505.7	70.474	4.057	0.560	-0.025	-0.027
Evader	7016.0	57.296	0.000	0.000	0.068	0.000

Table I. Initial Conditions

thrust can only go from zero to the maximum value. For the minimizer, the thrust will be maximum when the switching function is negative and thrust will be zero when the switching function is positive. The thrust for the maximizer is determined in the same manner except the positive switching function produces maximum thrust and a negative switching function produces zero thrust. To avoid this bang-bang control, a thrust change constraint (AK) was used. The thrust change was the result of the switching function divided by AK. The value of 10^{-11} for AK was found to provide the best results. The smaller AK was, the larger was the thrust change, however, if the thrust change is too small, the thrust may never make any significant change. Values of 10^{-10} to 10^{-12} were used to produce the results shown in the following tables.

Discussion

The results shown in Tables II - XI are as anticipated, when the mass term is weighted more, the range decreases and the final mass increases. There are some cases, however, where the trend takes a sudden dip that is considerably greater then expected. This could be the result of many variables, but the primary one is that the convergence for that case was poor. Another possibility is that the thrust was not able to change fast enough. The average value of the switching function is around 10^{-11}, although in some cases this value may vary considerably. If the thrust can only go from zero to the maximum value. For the minimizer, the thrust will be maximum when the switching function is negative and thrust will be zero when the switching function is positive. The thrust for the maximizer is determined in the same manner except the positive switching function produces maximum thrust and a negative switching function produces zero thrust. To avoid this bang-bang control, a thrust change constraint (AK) was used. The thrust change was the result of the switching function divided by AK. The value of 10^{-11} for AK was found to provide the best results. The smaller AK was, the larger was the thrust change, however, if the thrust change is too small, the thrust may never make any significant change. Values of 10^{-10} to 10^{-12} were used to produce the results shown in the following tables.

Discussion

The results shown in Tables II - XI are as anticipated, when the mass term is weighted more, the range decreases and the final mass increases. There are some cases, however, where the trend takes a sudden dip that is considerably greater then expected. This could be the result of many variables, but one possibility is that the convergence for that case was poor. Another possibility is that the thrust was not able to change fast enough. The average value of the switching function is around 10^{-11}, although in some cases this value may vary considerably. If the switching function changes considerably, then the thrust change will be too great or too small. The use of the AK parameter was designed to smooth out the rapid switching caused by a switching function of very small magnitude which could vary from positive to negative values due to errors in computing the components. If the switching function is extremely small, some of its components are even smaller and the chance of a sign error as a result of additive errors exists. The use of the AK parameter was designed to reduce the effect of this error, yet it may also reduce the optimality of the thrust change. Another possible method is to allow the thrust to switch rapidly or by some preselected amount per iteration unless the magnitude of the switching function is less then some very small value. When the small magnitude check is satisfied, the use of an AK type of parameter may be useful.

AK $(x10^{-11})$	Fmc $(x10^{-3})$	Range (NM)	Mass (Slugs)
0.1	0.0	6.314	1035.0887
0.1	2.0	0.217	949.3241
1.0	0.0	5.618	1068.9366
1.0	0.8	3.199	1097.3665
1.0	2.0	0.484	1101.2084
1.0	4.0	6.325	1192.1009
10.0	2.0	2.251	1045.7356

Table II. Case 1 and Near Optimal Pursuer

AK $(x10^{-11})$	Fmc $(X10^{-3})$	Range (NM)	Mass (Slugs)
0.1	0.0	45.231	1080.0531
0.1	2.0	34.577	1199.8874
1.0	0.0	55.383	1008.3273
1.0	0.8	48.478	1063.1035
1.0	2.0	45.831	1096.6912
1.0	4.0	39.540	1149.7747
10.0	2.0	57.237	1079.0888

Table III. Case 1 and Non-Optimal Pursuer

AK ($x10^{-11}$)	Fmc ($x10^{-3}$)	Range (NM)	Mass (Slugs)
0.1	0.0	5.168	1077.9560
0.1	2.0	1.919	1234.9775
1.0	0.0	2.90	1083.7555
1.0	0.8	0.636	1036.3445
1.0	2.0	2.113	994.8289
1.0	4.0	2.162	1250.0000
10.0	2.0	1.808	1130.7665

Table IV. Case 2 and Near Optimal Pursuer

AK ($x10^{-11}$)	Fmc ($x10^{-3}$)	Range (NM)	Mass (Slugs)
0.1	0.0	55.272	1082.7480
0.1	2.0	39.517	1250.0000
1.0	0.0	55.189	1085.3884
1.0	0.8	52.378	1114.7330
1.0	2.0	45.937	1181.1390
1.0	4.0	39.517	1250.0000
10.0	2.0	49.715	1129.5821

Table V. Case 2 and Non-Optimal Pursuer

AK ($x10^{-11}$)	Fmc ($x10^{-3}$)	Range (NM)	Mass (Slugs)
0.1	0.0	6.627	1077.7022
0.1	2.0	0.768	1239.9775
1.0	0.0	3.712	1083.9067
1.0	0.8	0.549	1098.7667
1.0	2.0	1.303	993.9869
1.0	4.0	0.557	1244.9887
10.0	2.0	2.576	1130.9590

Table VI. Case 3 and Near Optimal Pursuer

AK ($x10^{-11}$)	Fmc ($x10^{-3}$)	Range (NM)	Mass (Slugs)
0.1	0.0	55.870	1082.6532
0.1	2.0	40.091	1250.0000
1.0	0.0	55.786	1085.4122
1.0	0.8	53.029	1114.2273
1.0	2.0	46.572	1181.4098
1.0	4.0	40.091	1250.0000
10.0	2.0	50.294	1129.9751

Table VII. Case 3 and Non-Optimal Pursuer

AK ($\times 10^{-11}$)	Fmc ($\times 10^{-3}$)	Range (NM)	Mass (Slugs)
0.0	0.0	13.238	1078.1804
0.1	2.0	0.305	1250.00
1.0	0.0	8.146	1092.9568
1.0	0.8	2.291	1135.758-
1.0	2.0	4.092	1035.4466
1.0	4.0	2.275	1250.00
10.0	2.0	5.879	1111.9201

Table VIII. Case 4 and Near Optimal Pursuer

AK ($\times 10^{-11}$)	Fmc ($\times 10^{-3}$)	Range (NM)	Mass (Slugs)
0.1	0.0	53.233	1088.8661
0.1	2.0	38.374	1250.00
1.0	0.0	49.234	1149.4164
1.0	0.8	51.850	1129.7944
1.0	2.0	46.772	1167.8777
1.0	4.0	38.374	1250.00
10.0	2.0	51.500	1118.0301

Table IX. Case 4 and Non-Optimal Pursuer

AK ($x10^{-11}$)	Fmc ($x10^{-3}$)	Range (NM)	Mass (Slugs)
0.1	0.0	21.159	922.6761
0.1	2.0	20.967	944.3129
1.0	0.0	21.168	922.6502
1.0	0.8	21.168	932.9685
1.0	2.0	21.161	925.7350
1.0	4.0	20.948	945.7547
10.0	2.0	17.396	922.8219

Table X. Case 5 and Near Optimal Pursuer

AK ($x10^{-11}$)	Fmc ($x10^{-3}$)	Range (NM)	Mass (Slugs)
0.1	0.0	31.916	1038.2526
0.1	2.0	22.848	1149.7747
1.0	0.0	37.452	990.1154
1.0	0.8	34.698	1026.0931
1.0	2.0	30.030	1086.2113
1.0	4.0	25.099	1146.7747
10.0	2.0	37.619	1002.7996

XI. Case 5 and Non-Optimal Pursuer

V. Conclusions

The data indicate a small fuel savings when using a Fmc other than o.o. There is also the anticipated reduction in the final range. The usefulness of this method is therefore dependent on the mission.

A mission requiring fuel only for evasive maneuvering would probably not use this near optimal control scheme. A mission that requires fuel for orbital maneuvering, station keeping, or long duration multiple evasions could gain some fuel savings with this near optimal scheme.

Further study could make the program more efficient. The scheme could also be tested against a variety of pursuers. Optimization of the various parameters in the scheme could then be attempted. This study has shown that a near optimal control scheme for an evading spacecraft can be used to produce a minimum fuel savings.

Bibliography

1. Isaacs, R., Differential Games. New York, New York: John Wiley and Sons, 1965.

2. Jacobson, D. H. and D. Q. Mayne, Differential Dynamic Programming, New York, New York: American Elsevier Publishing Company, Inc., 1970.

3. Anderson, G. M. and G. D. Bohn, "A near-Optimal Control Law for Pursuit-Evasion Problems Between Two Spacecraft." AIAA Paper No. 76-794, presented at AIAA/AAS Astrodynamics Conference, San Diego, California, Aug 16-18, 1976.

4. Bryson, A. E. and Y. C. Ho, Applied Optimal Control, Waltham, Massachusetts: Blaisdell Company, 1969.

5. Anderson, G. M., "A Transition Matrix Method for Generating Near Optimal Closed-Loop Solutions to Non-linear Zero-Sum Differential Games," International Journal of System Sciences, Vol. 7, May 1976, pp. 529-543.

6. Anderson, G. M., "A near-Optimal Closed-Loop Solution Method for Non-singular Zero-Sum Differential Games," Journal of Optimization Theory and Applications, Vol. 18, March 1974, pp. 303-318.

7. Jarmark, B.S.A., A New Convergence Control Technique in Differential Dynamic Programming, Report TRITA-REG-7502, The Royal Institute of Technology, Dept. of Automatic Control, Stockholm, Sweden.

8. Anderson, G. M., "Feedback Control for Pursuit-Evasion Problems Between Two Spacecraft Based on Differential Dynamic Programming." Paper No. 77-44, presented at 15th Aerospace Sciences Meeting, Los Angeles, California, Jan 24-26, 1977.

Appendix A

Optimality Conditions

The optimality conditions are found by taking the partial derivative of the Hamiltonian with respect to the controls. Solving for the controls results in a choice of positive or negative values. The decision of which value to use is based on the second partial derivative of the Hamiltonian with respect to the controls. This is based on the assumption that the Hamiltonian is separable which it is in this case if

$$H = \lambda_e^T \dot{x}_e + \lambda_p^T \dot{x}_p \tag{A-1}$$

Since

$$\frac{\partial}{\partial v}\left(\lambda_p^T \dot{x}_p\right) = \frac{\partial}{\partial u}\left(\lambda_e^T \dot{x}_e\right) = 0 \tag{A-2}$$

then

$$H_v = \frac{\partial}{\partial v}\left(\lambda_e^T \dot{x}_e\right) = 0 \tag{A-3}$$

$$H_u = \frac{\partial}{\partial u}\left(\lambda_p^T \dot{x}_p\right) = 0 \tag{A-4}$$

and

$$H_{vv} = \frac{\partial^2}{\partial v_i \partial v_j}\left(\lambda_e^T \hat{x}_e\right) \leq 0 \tag{A-5}$$

$$H_{uu} = \frac{\partial^2}{\partial u_i \partial u_j} \left(\lambda_p^T \dot{x}_p\right) \geq 0 \qquad \text{(A-6)}$$

Solving Eq. (A-3)

$$\left[(\lambda_{v_r e} \cos\alpha_1 + \lambda_{v_\phi e} \sin\alpha_1)\cos\alpha_2 + \lambda_{v_\theta e} \sin\alpha_2 - 1/C_e\right]/m = 0 \qquad \text{(A-7)}$$

$$T/m \left[\cos\alpha_2 \left(-\lambda_{v_r e} \sin\alpha_1 + \lambda_{v_\phi e} \cos\alpha_1\right)\right] = 0 \qquad \text{(A-8)}$$

$$T/m\left[-\sin\alpha_2 (\lambda_{v_r e} \cos\alpha_1 + \lambda_{v_\phi e} \sin\alpha_1) + \lambda_{v_\theta e} \cos\alpha_2\right] = 0 \qquad \text{(A-9)}$$

Since $\cos\alpha_2 \geq 0$ the bracket term must be equal to zero.

$$\frac{\lambda_{v_\phi e}}{\lambda_{v_r e}} = \frac{\sin\alpha_1}{\cos\alpha_1} \qquad \text{(A-10)}$$

or

$$\sin\alpha_1 = \pm \lambda_{v_\phi e} / \left(\lambda^2_{v_r e} + \lambda^2_{v_\phi e}\right)^{1/2} \qquad \text{(A-11)}$$

$$\cos\alpha_1 = \pm \lambda_{v_r e} / \left(\lambda^2_{v_r e} + \lambda^2_{v_\phi e}\right)^{1/2} \qquad \text{(A-12)}$$

To decide which sign to use solve Eq (A-5)

$$0 \leq 0 \qquad \text{(A-13)}$$

$$\cos\alpha_2 (-\lambda_{v_r e} \cos\alpha_1 - \lambda_{v_\phi e} \sin\alpha_1)\ T/m \leq 0 \qquad \text{(A-14)}$$

$$\left[-\cos\alpha_2 (\lambda_{v_r e} \cos\alpha_1 + \lambda_{v_\phi e} \sin\alpha_1) - \lambda_{v_\theta e} \sin\alpha_2\right] T/m \leq 0 \qquad \text{(A-15)}$$

then substituting Eqs. (A-11) and (A-12) into (A-14)

$$\cos\alpha_2 \left\{ -\lambda_{v_r}^{e}\left[\frac{\pm\lambda_{v_r}^{e}}{\left(\lambda_{v_r}^{e\,2} + \lambda_{v_\phi}^{e\,2}\right)^{1/2}}\right] - \lambda_{v_\phi}^{e}\left[\frac{\pm\lambda_{v_\phi}^{e}}{\left(\lambda_{v_r}^{e\,2} + \lambda_{v_\phi}^{e\,2}\right)^{1/2}}\right]\right\} T/m \leq 0 \qquad \text{(A-16)}$$

By choosing the positive sign in Eqs. (A-11) and (A-12) we insure that Eq. (A-16) is satisfied. Substituting into Eq. (A-9) and solving for α_2

$$\left\{ -\sin\alpha_2\left[\frac{\lambda_{v_r}^{e\,2} + \lambda_{v_\phi}^{e\,2}}{\left(\lambda_{v_r}^{e\,2} + \lambda_{v_\phi}^{e\,2}\right)^{1/2}}\right] + \lambda_{v_\theta}^{e}\cos\alpha_2 \right\} T/m = 0 \qquad \text{(A-17)}$$

or

$$\sin\alpha_2/\cos\alpha_2 = \lambda_{v_\theta}^{e}\Big/\left[\left(\lambda_{v_r}^{e\,2} + \lambda_{v_\phi}^{e\,2}\right)\Big/\left(\lambda_{v_r}^{e\,2} + \lambda_{v_\phi}^{e\,2}\right)^{1/2}\right] \qquad \text{(A-18)}$$

$$\sin\alpha_2 = \pm\lambda_{v_\theta}^{e}\Big/\left(\lambda_{v_r}^{e\,2} + \lambda_{v_\phi}^{e\,2} + \lambda_{v_\theta}^{e\,2}\right)^{1/2} \qquad \text{(A-19)}$$

$$\cos\alpha_2 = \left[\pm\left(\lambda_{v_r}^{e\,2} + \lambda_{v_\phi}^{e\,2}\right)\Big/\left(\lambda_{v_r}^{e\,2} + \lambda_{v_\phi}^{e\,2}\right)^{1/2}\right]\Big/\left(\lambda_{v_r}^{e\,2} + \lambda_{v_\phi}^{e\,2} + \lambda_{v_\theta}^{e\,2}\right)^{1/2} \qquad \text{(A-20)}$$

Substituting into Eq. (A-15)

$$\left[\frac{\mp\left(\lambda_{v_r}^{e\,2} + \lambda_{v_\phi}^{e\,2}\right)^2\Big/\left(\lambda_{v_r}^{e\,2} + \lambda_{v_\phi}^{e\,2}\right) \mp \lambda_{v_\theta}^{e\,2}}{\left(\lambda_{v_r}^{e\,2} + \lambda_{v_\phi}^{e\,2} + \lambda_{v_\theta}^{e\,2}\right)^{1/2}}\right] T/m \leq 0 \qquad \text{(A-21)}$$

By choosing the positive sign in Eqs. (A-19) and (A-20) we insure that Eq. (A-21) is satisfied. For the optimality conditions on the pursuer the same equations are used except that Eqs. (A-15) and (A-16) result in a requirement for greater than or equal to zero instead of the less than or equal to requirement for the evader. This changes the signs on the cosine and sine functions so that

$$\sin\alpha_1 = -\lambda_{v_\phi p} / (\lambda^2_{v_r p} + \lambda^2_{v_\phi p})^{1/2} \tag{A-22}$$

$$\cos\alpha_1 = -\lambda_{v_r p} / (\lambda^2_{v_r p} + \lambda^2_{v_\phi p})^{1/2} \tag{A-23}$$

and

$$\sin\alpha_2 = -\lambda_{v_\theta p} / (\lambda^2_{v_r p} + \lambda^2_{v_\phi p} + \lambda^2_{v_\theta p})^{1/2} \tag{A-24}$$

$$\cos\alpha_2 = -(\lambda^2_{v_r p} + \lambda^2_{v_\phi p})^{1/2} / (\lambda^2_{v_r p} + \lambda^2_{v_\phi p} + \lambda^2_{v_\theta p})^{1/2} \tag{A-25}$$

APPENDIX B

PLOTS OF TRAJECTORIES

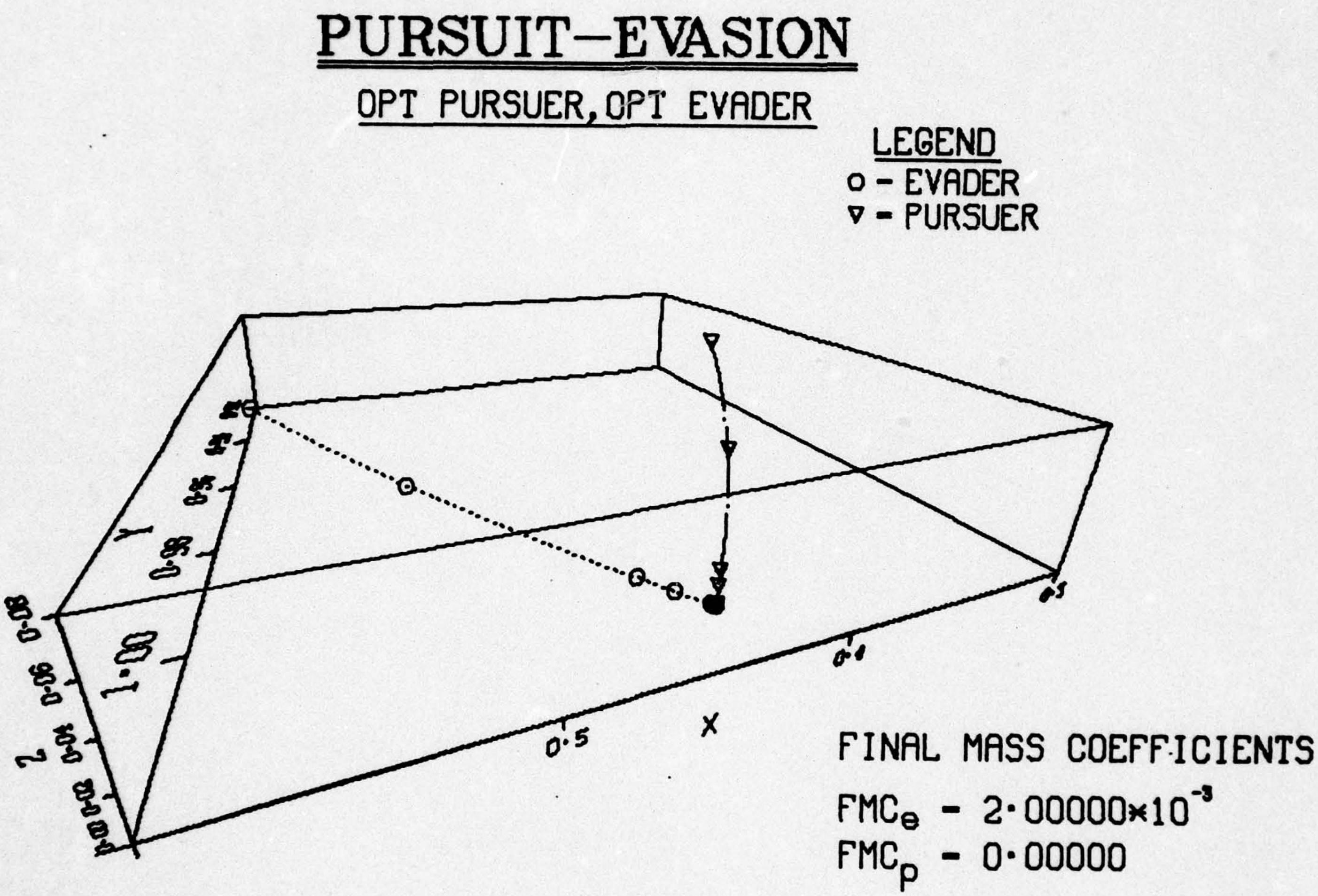

Fig. B-1 Case 1 AK = 0.1×10^{-11}

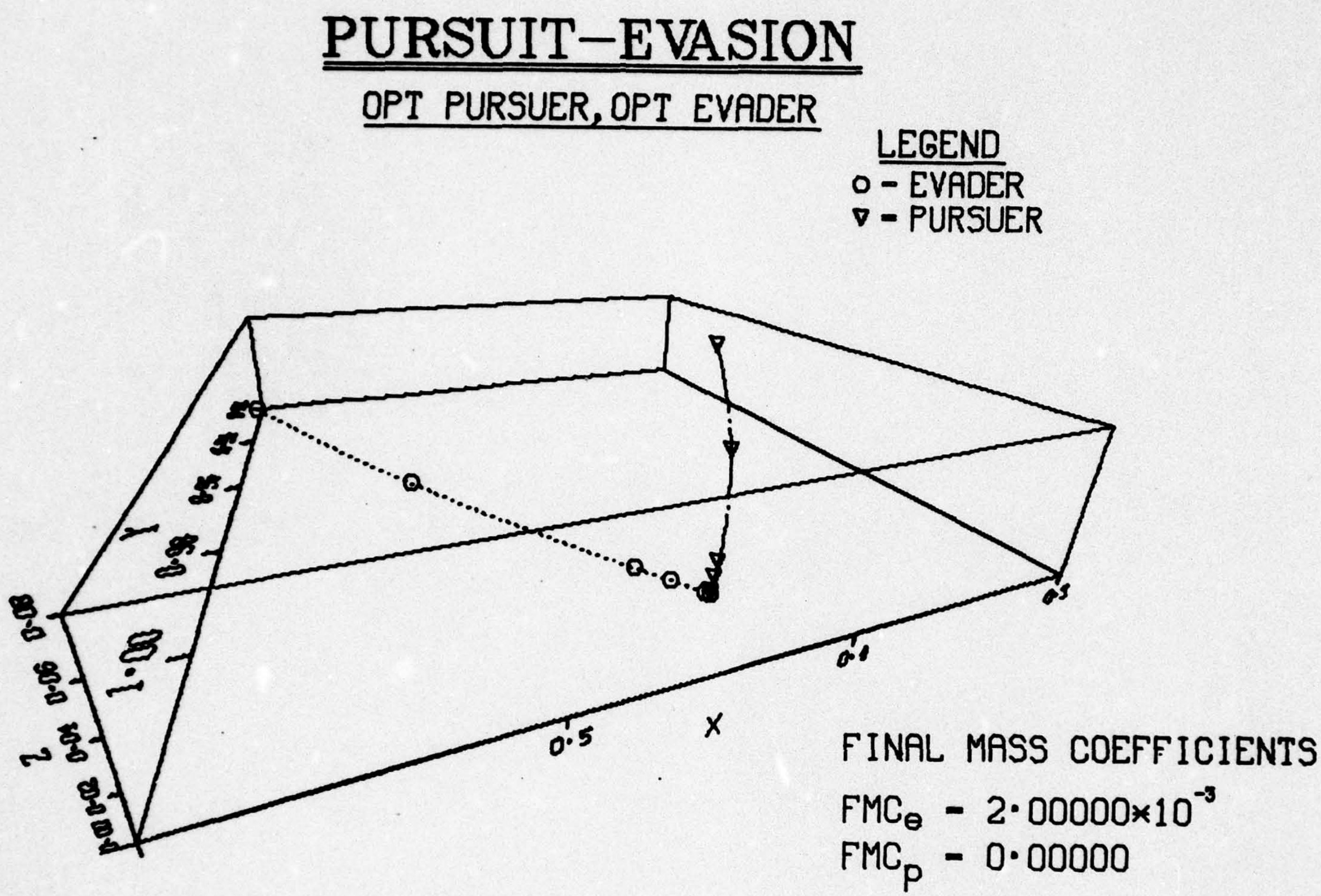

Fig. B-2 Case 1 AK = 1.0 X 10^{-11}

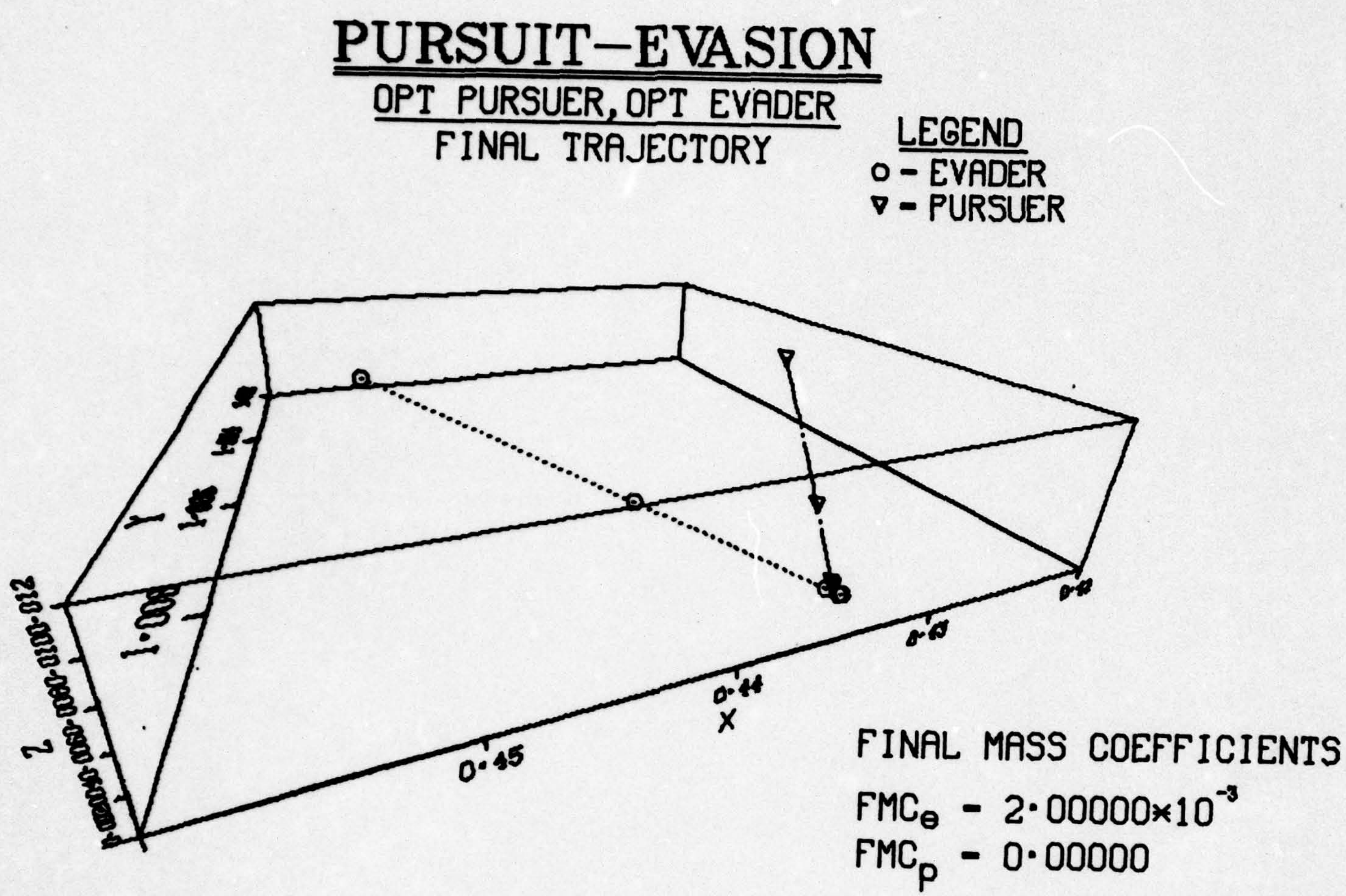

Fig. B-3 Case 1 AK = 1.0×10^{-11}

PURSUIT–EVASION

OPT PURSUER, OPT EVADER

LEGEND
o - EVADER
▽ - PURSUER

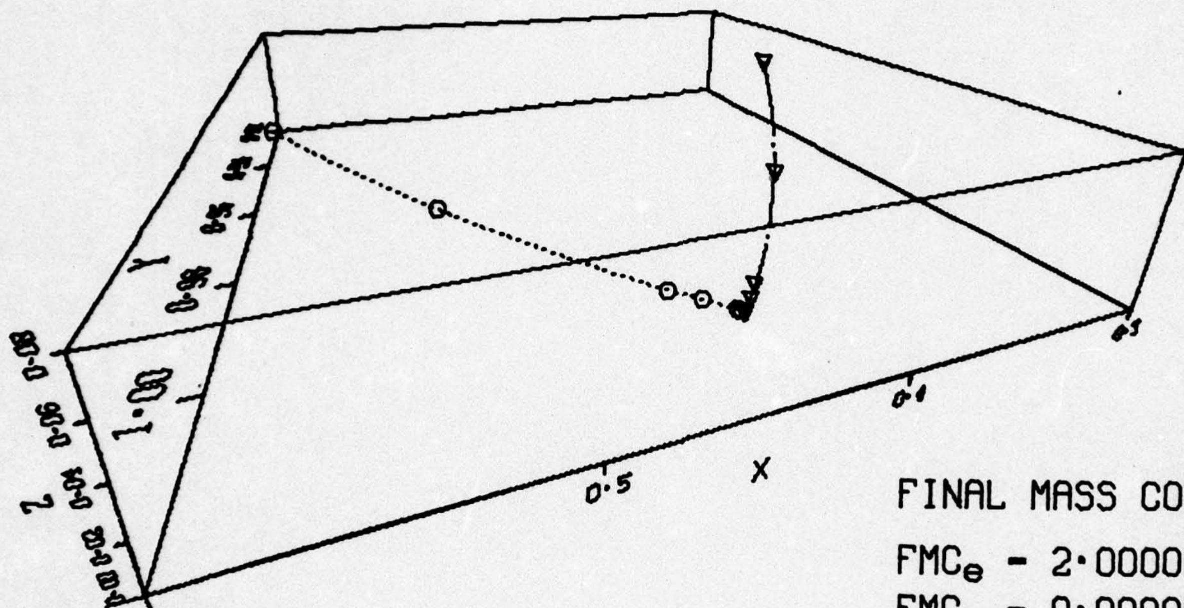

FINAL MASS COEFFICIENTS

FMC_e - $2 \cdot 00000 \times 10^{-3}$
FMC_p - $0 \cdot 00000$

Fig. B-4 Case 1 AK = 10.0×10^{-11}

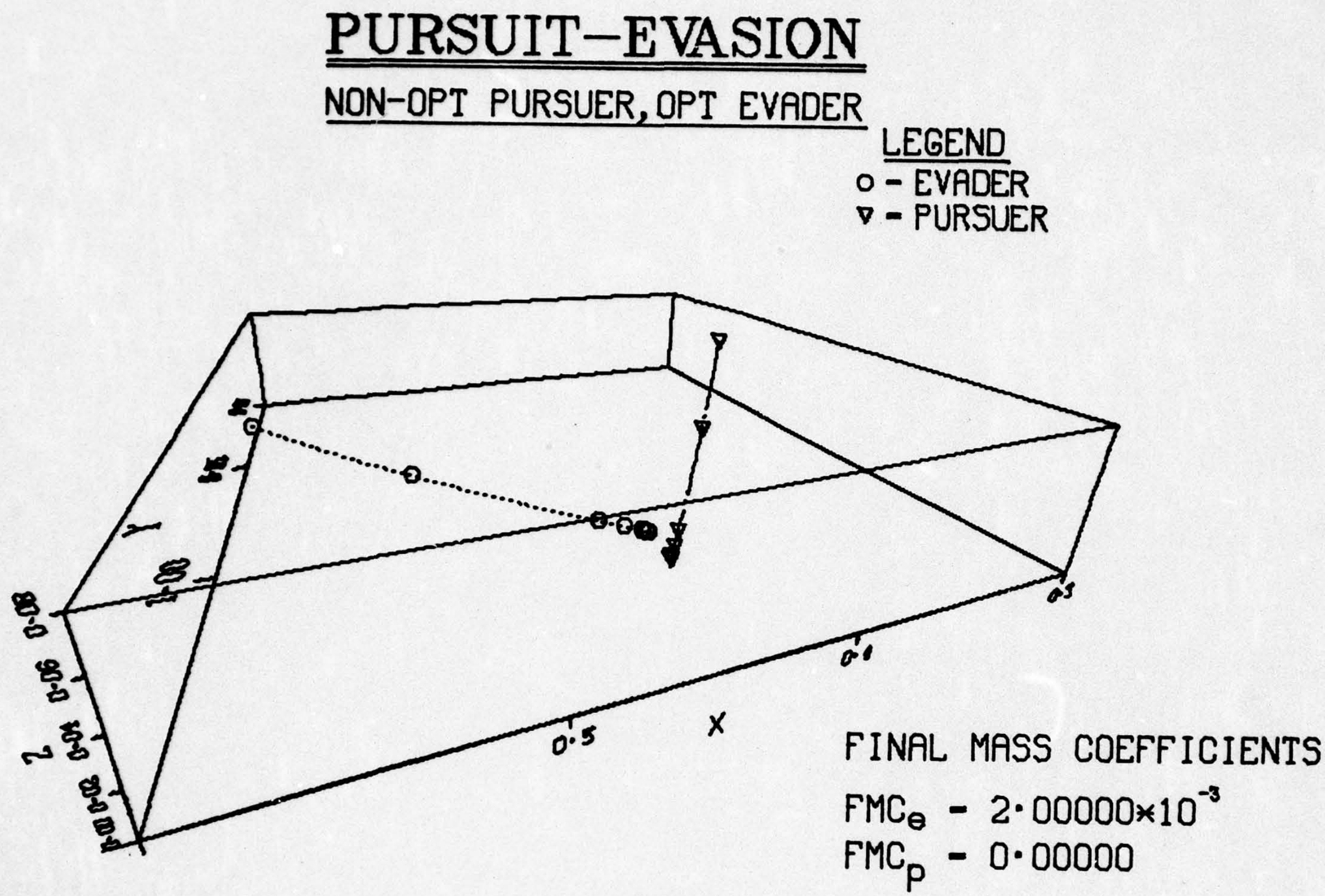

Fig. B-5 Case 1 AK = 0.1 X 10^{-11}

PURSUIT–EVASION

NON-OPT PURSUER, OPT EVADER

LEGEND
o - EVADER
▽ - PURSUER

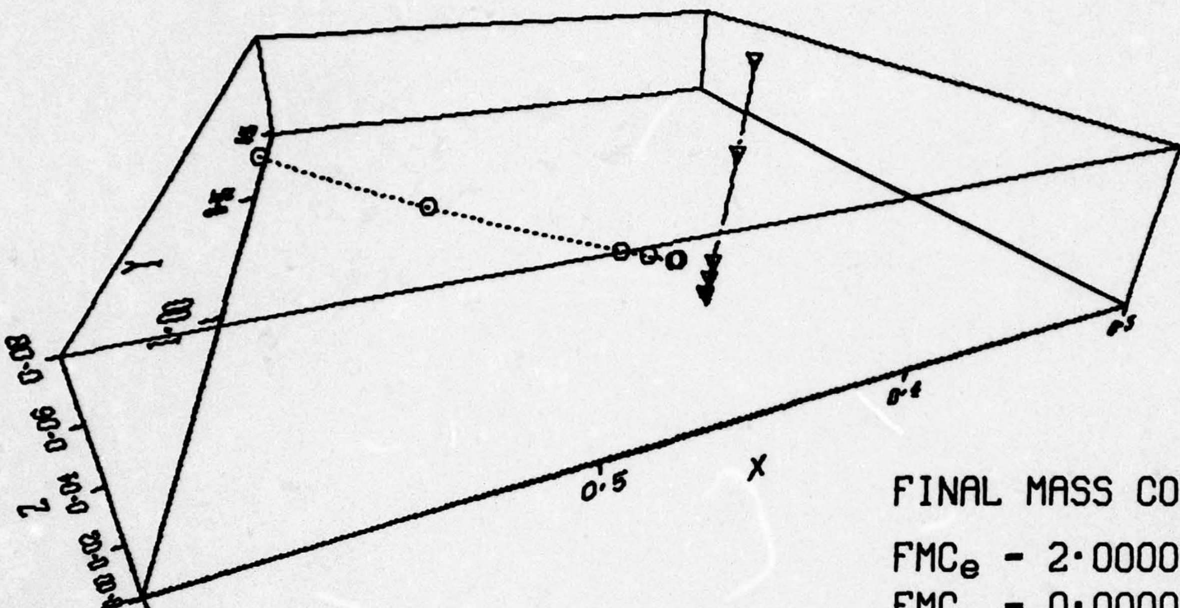

FINAL MASS COEFFICIENTS

FMC_e - $2 \cdot 00000 \times 10^{-3}$
FMC_p - $0 \cdot 00000$

Fig. B-6 Case 1 AK = 1.0×10^{-11}

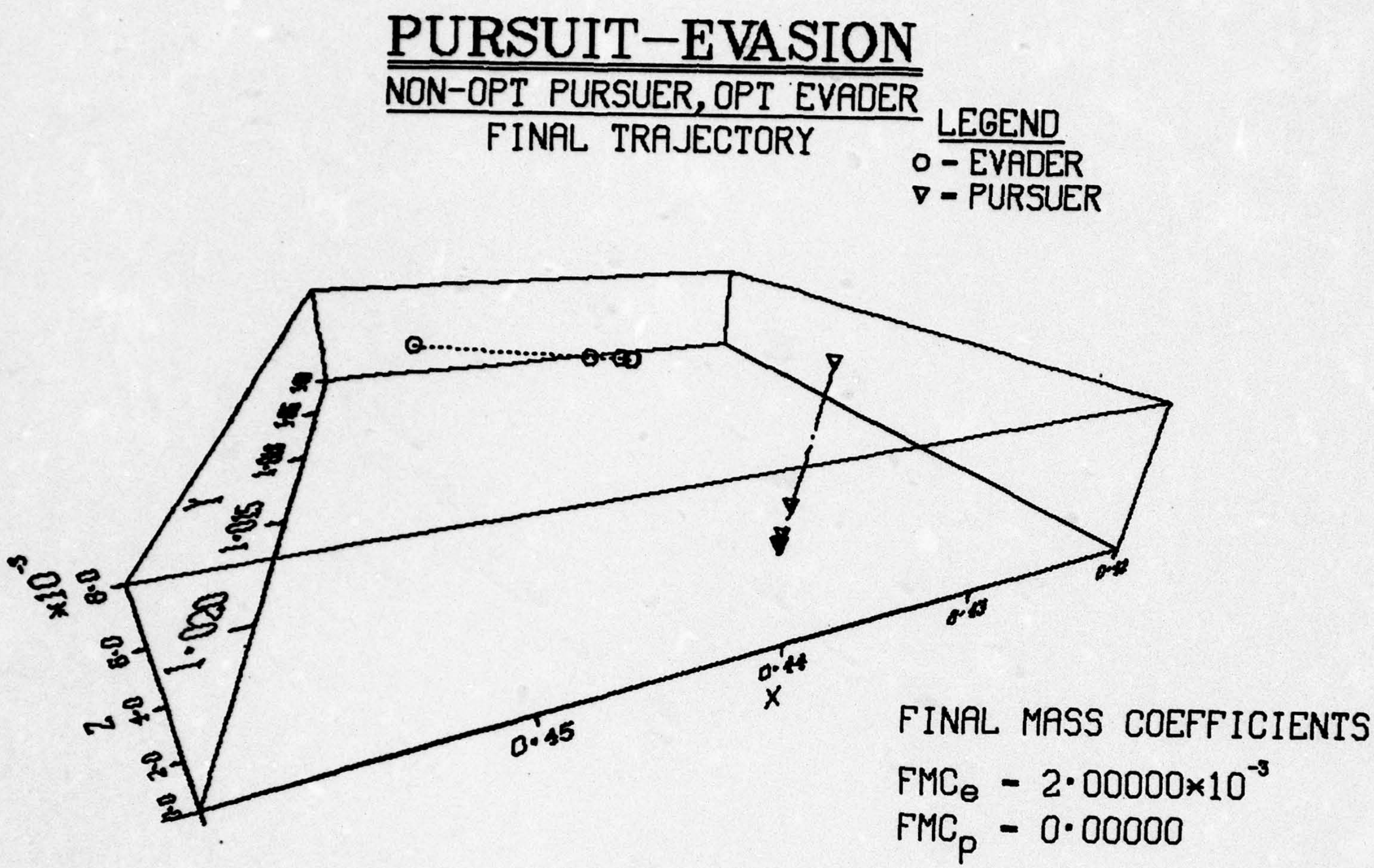

Fig. B-7 Case 1 AK = 1.0 X 10^{-11}

PURSUIT–EVASION

NON-OPT PURSUER, OPT EVADER

LEGEND
o – EVADER
▽ – PURSUER

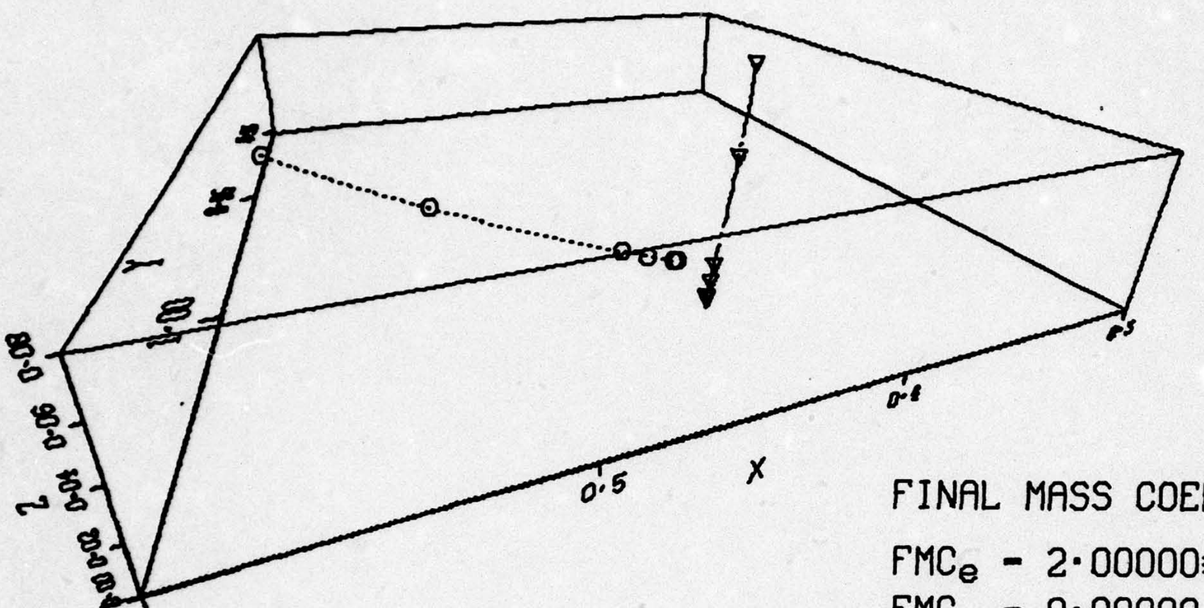

FINAL MASS COEFFICIENTS

FMC_e – 2.00000×10^{-3}
FMC_p – 0.00000

Fig. 8 Case 1 AK = 10.0×10^{-11}

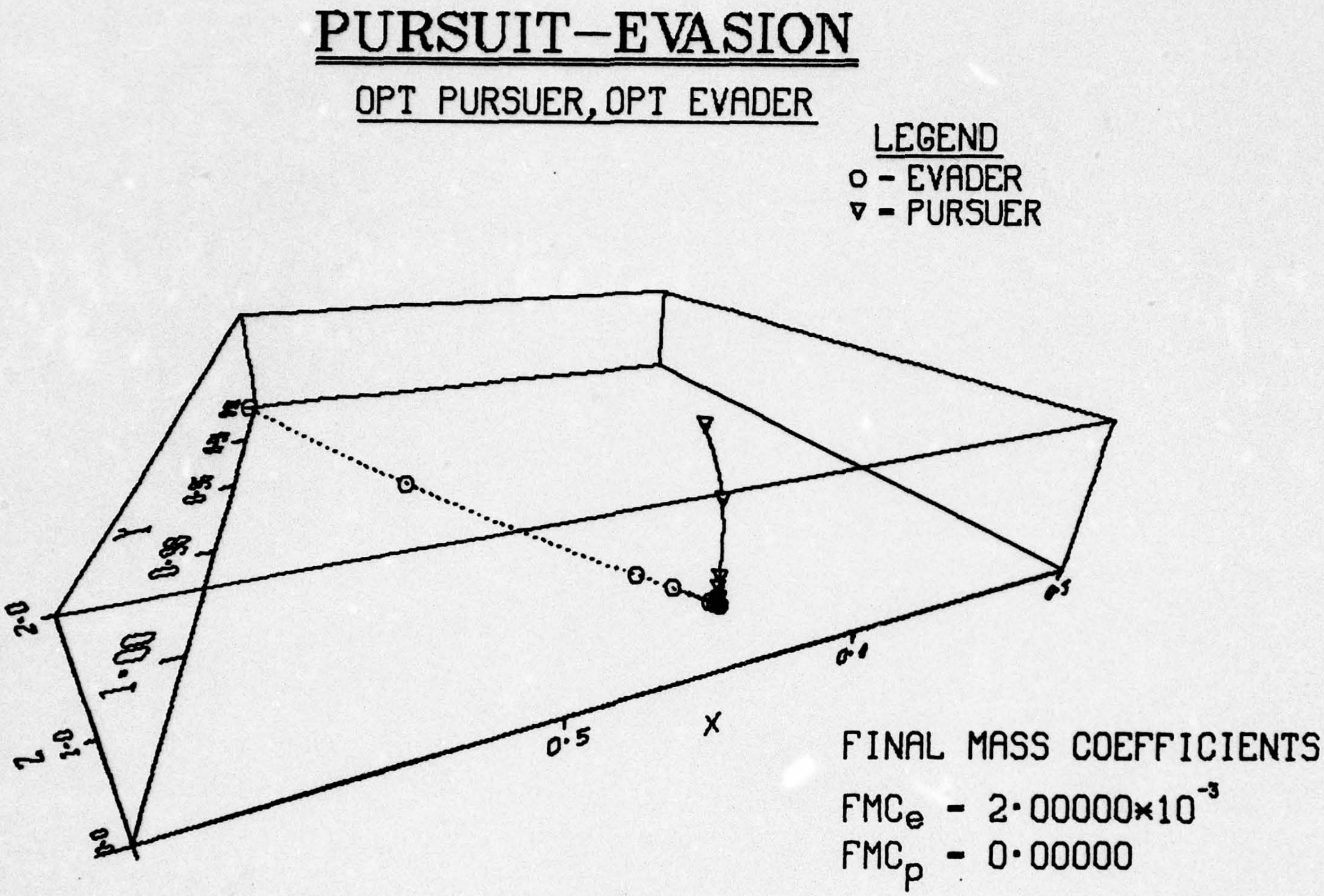

Fig. B-9 Case 2 AK = 0.1 X 10^{-11}

PURSUIT–EVASION

OPT PURSUER, OPT EVADER

LEGEND
o - EVADER
∇ - PURSUER

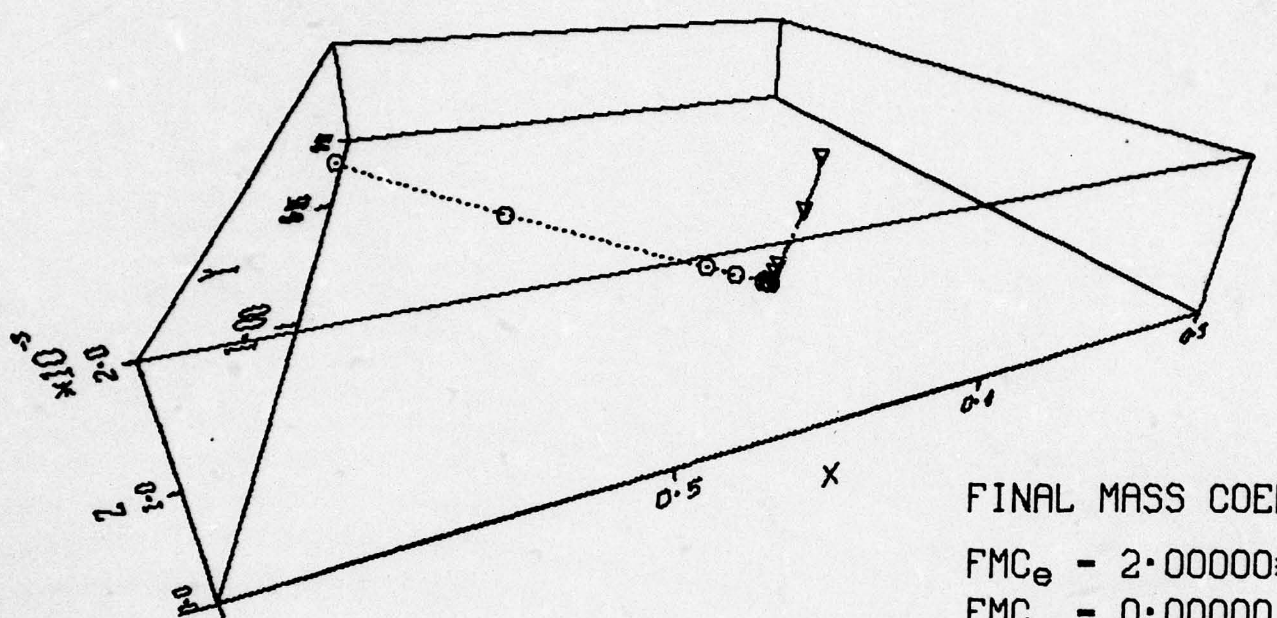

FINAL MASS COEFFICIENTS

FMC_e - 2.00000×10^{-3}
FMC_p - 0.00000

Fig. 10 Case 2 AK = 1.0×10^{-11}

PURSUIT–EVASION

OPT PURSUER, OPT EVADER

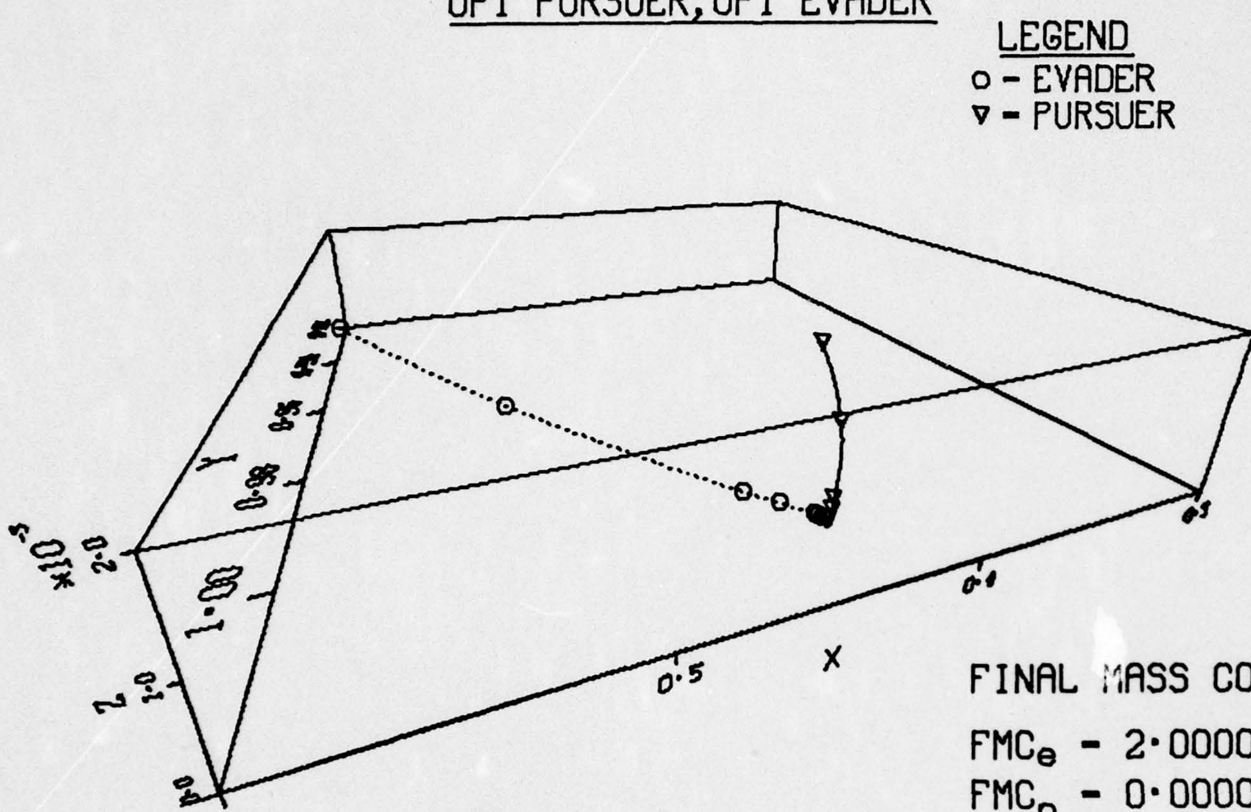

FINAL MASS COEFFICIENTS

FMC_e – $2 \cdot 00000 \times 10^{-3}$

FMC_p – $0 \cdot 00000$

Fig. B-11 Case 2 AK = 10.0 X 10^{-11}

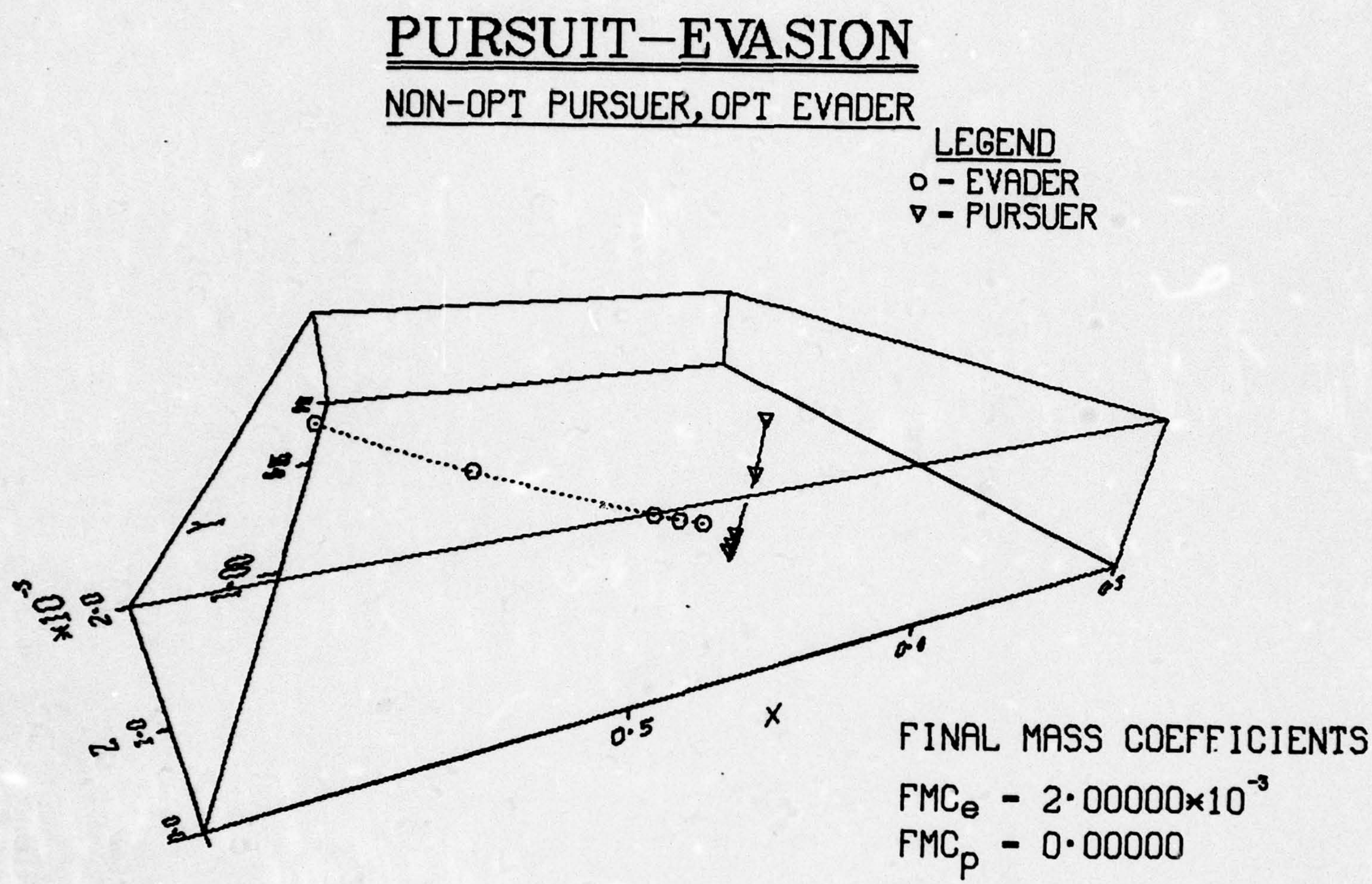

Fig. B-12 Case 2 AK = 0.1 X 10^{-11}

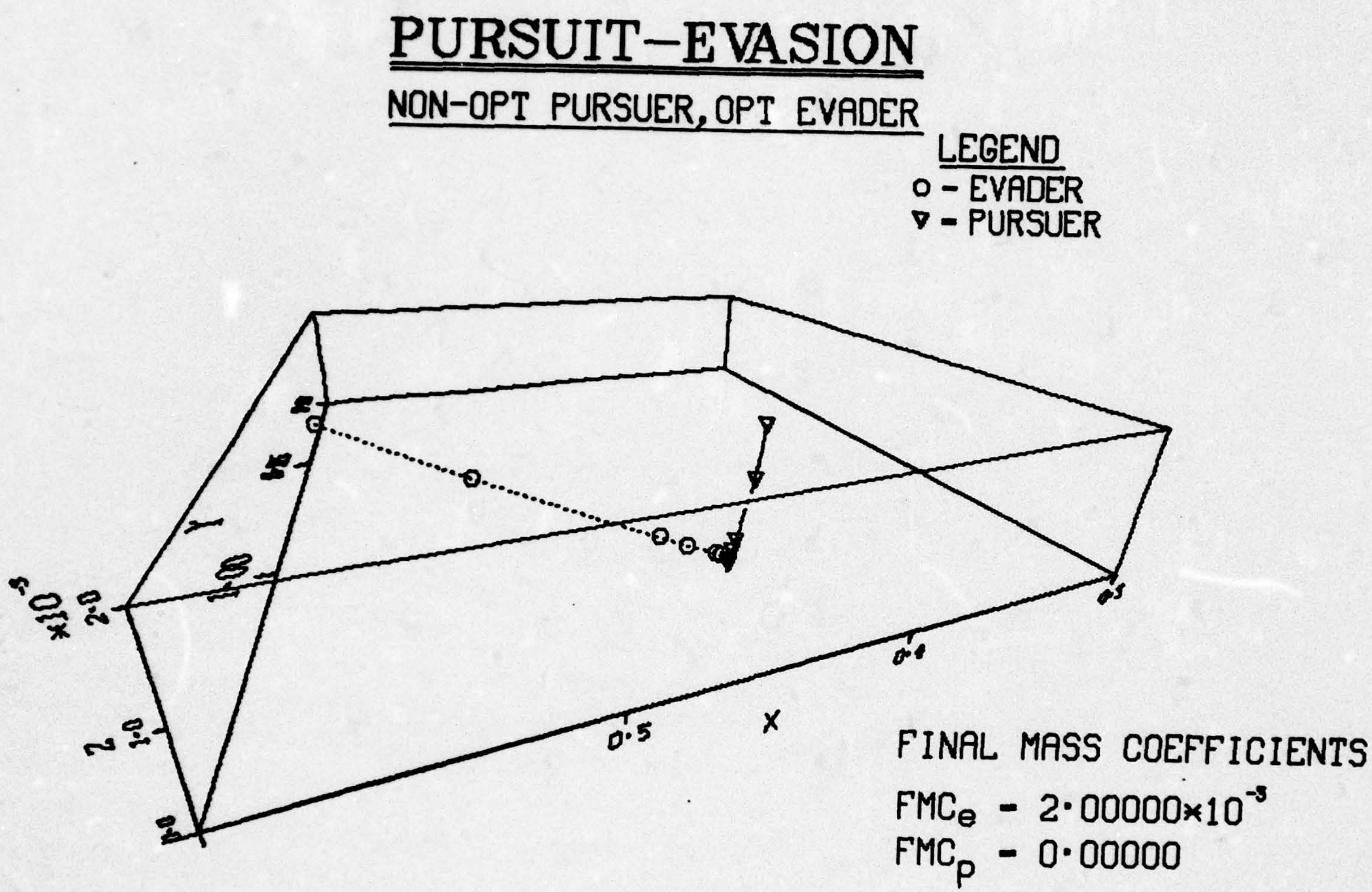

Fig. B-13 Case 2 AK = 1.0×10^{-11}

PURSUIT–EVASION

NON-OPT PURSUER, OPT EVADER

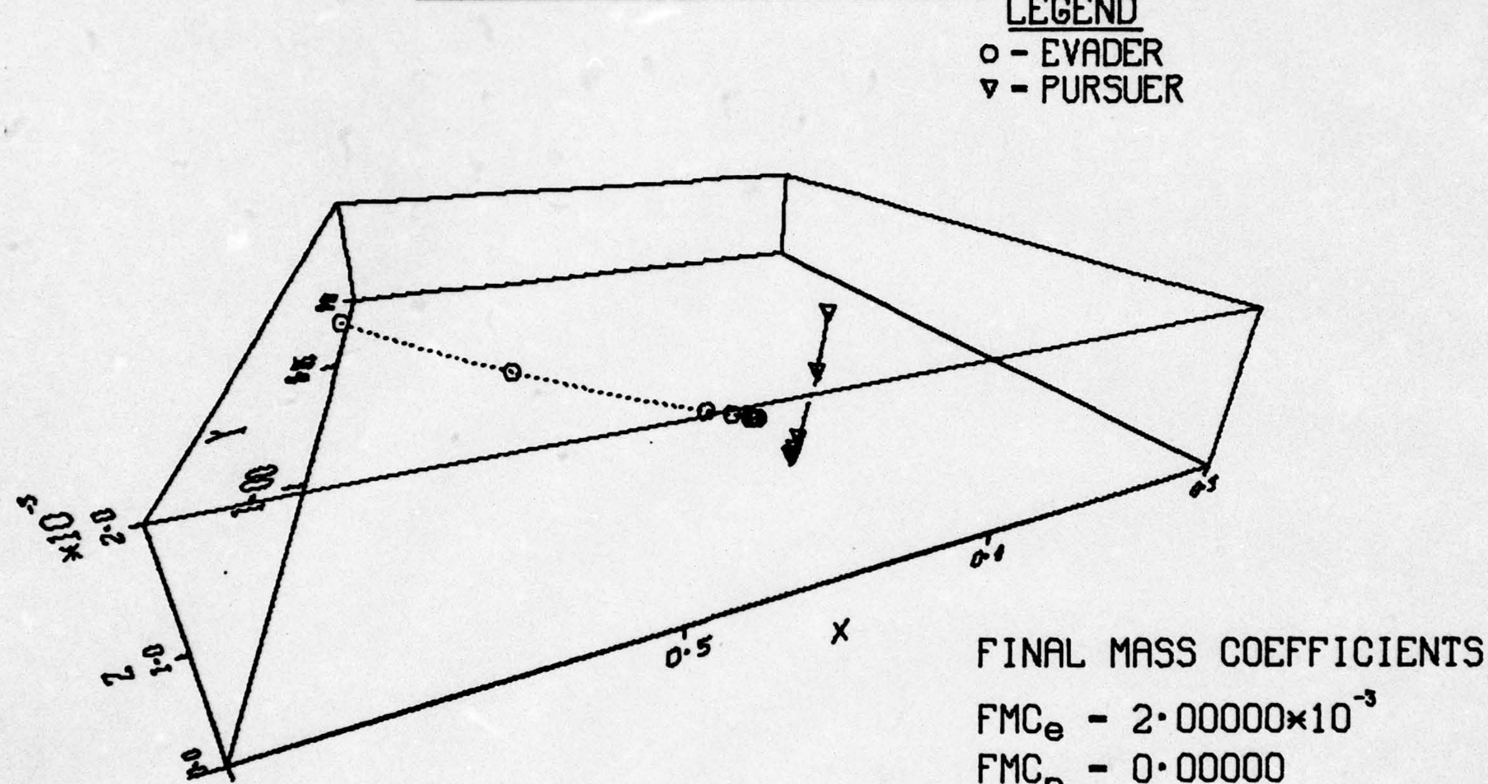

FINAL MASS COEFFICIENTS

FMC_e - $2\cdot00000\times10^{-3}$

FMC_p - $0\cdot00000$

Fig. B-14   Case 2   AK = 10.0×10^{-11}

PURSUIT–EVASION

OPT PURSUER, OPT EVADER

LEGEND
o - EVADER
▽ - PURSUER

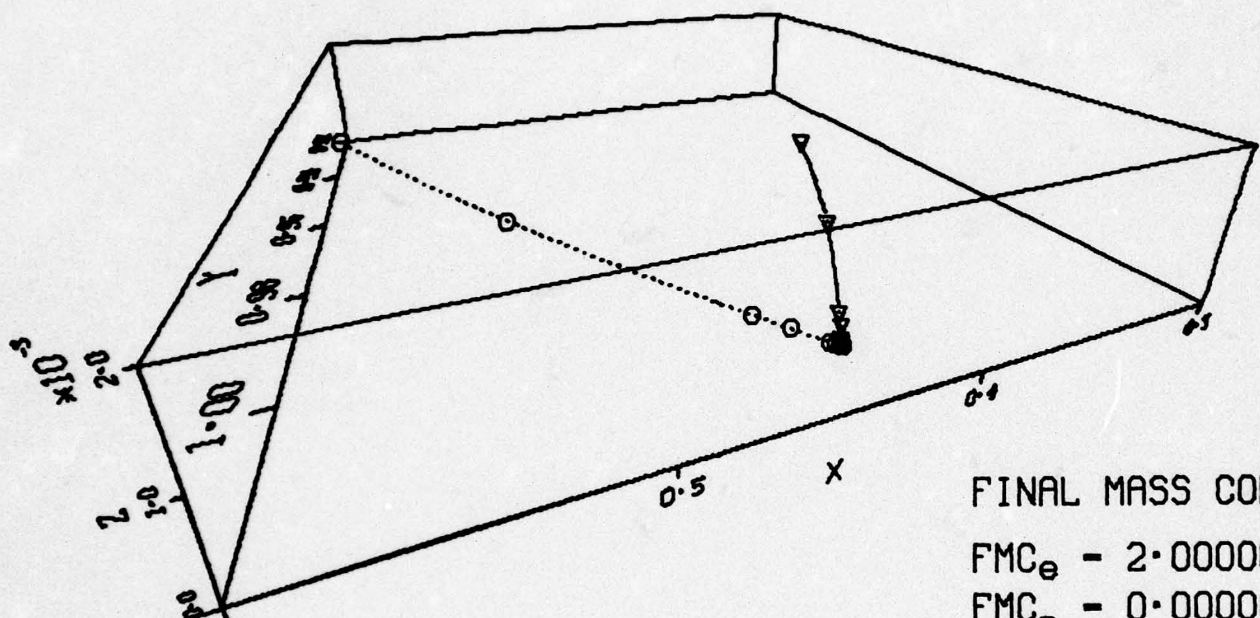

FINAL MASS COEFFICIENTS

FMC_e - $2{\cdot}00000 \times 10^{-3}$
FMC_p - $0{\cdot}00000$

Fig. B-15 Case 3 AK = 0.1×10^{-11}

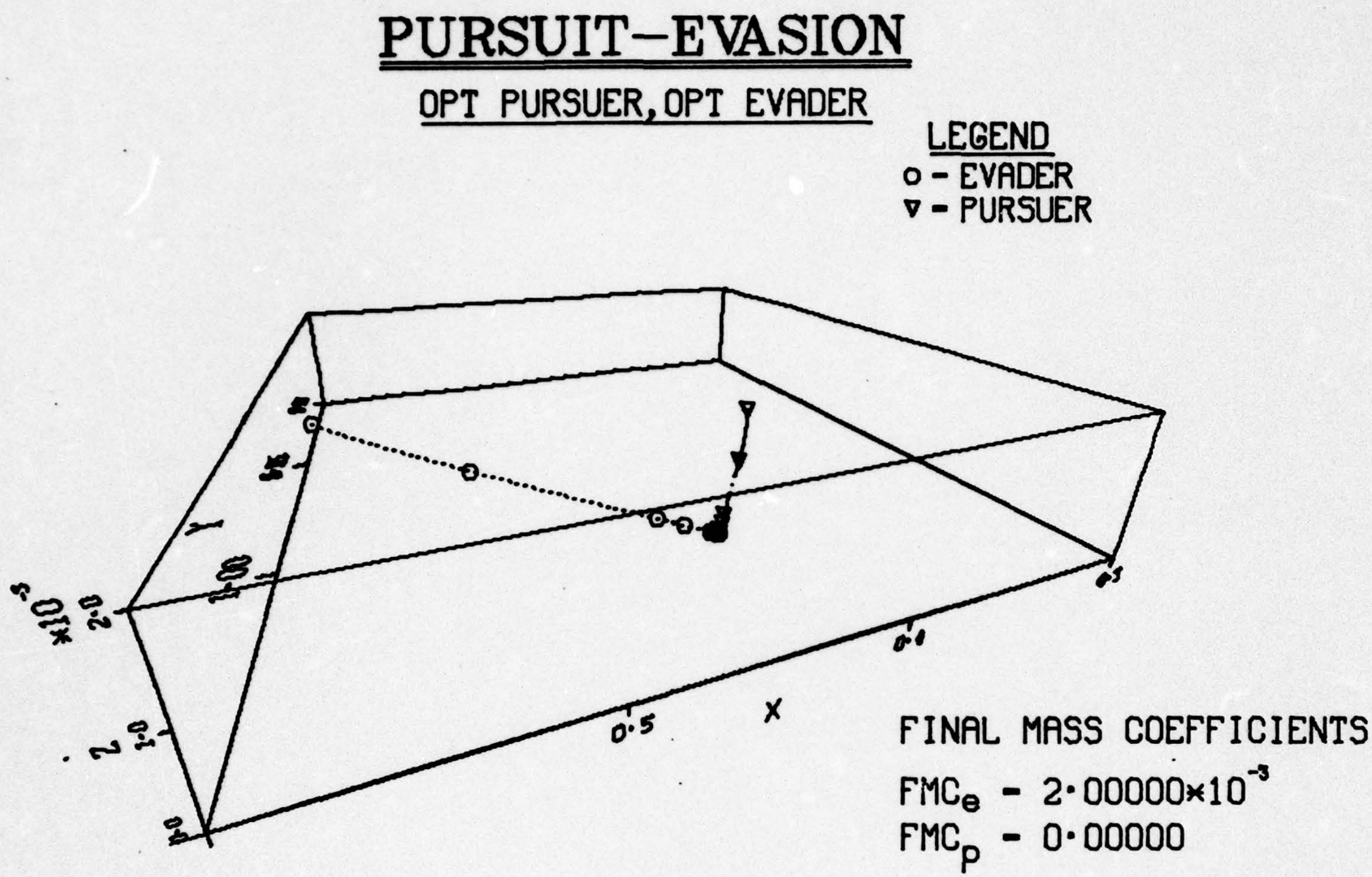

Fig. B-16 Case 3 AK = 1.0×10^{-11}

PURSUIT–EVASION

OPT PURSUER, OPT EVADER

LEGEND
o – EVADER
∇ – PURSUER

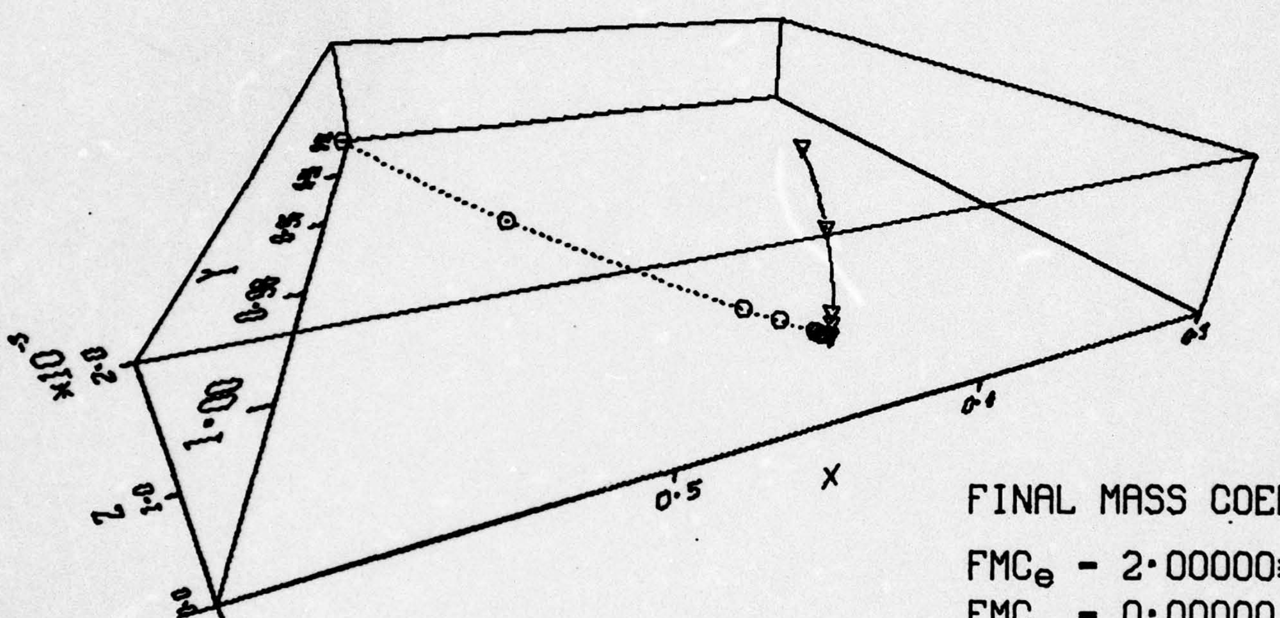

FINAL MASS COEFFICIENTS

FMC_e – $2 \cdot 00000 \times 10^{-3}$
FMC_p – $0 \cdot 00000$

Fig. B-17 Case 3 AK = 10.0×10^{-11}

PURSUIT—EVASION

NON-OPT PURSUER, OPT EVADER

LEGEND
o - EVADER
▽ - PURSUER

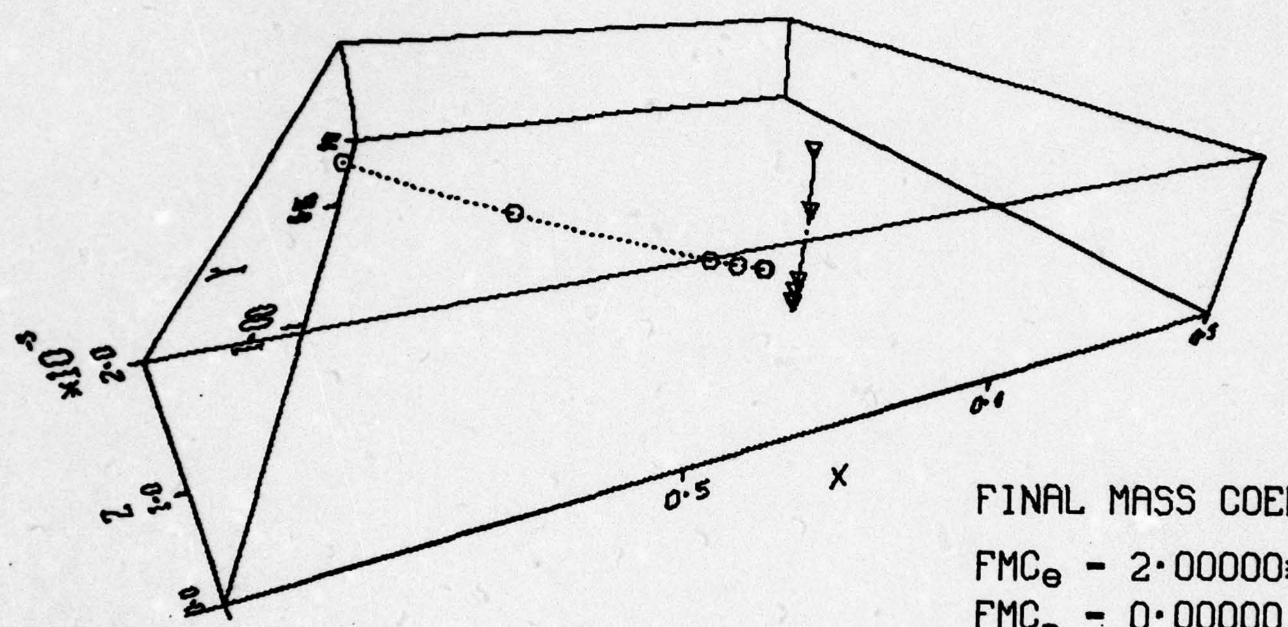

FINAL MASS COEFFICIENTS

FMC_e - $2\cdot00000\times10^{-3}$
FMC_p - $0\cdot00000$

Fig. B-18 Case 3 AK = 0.1×10^{-11}

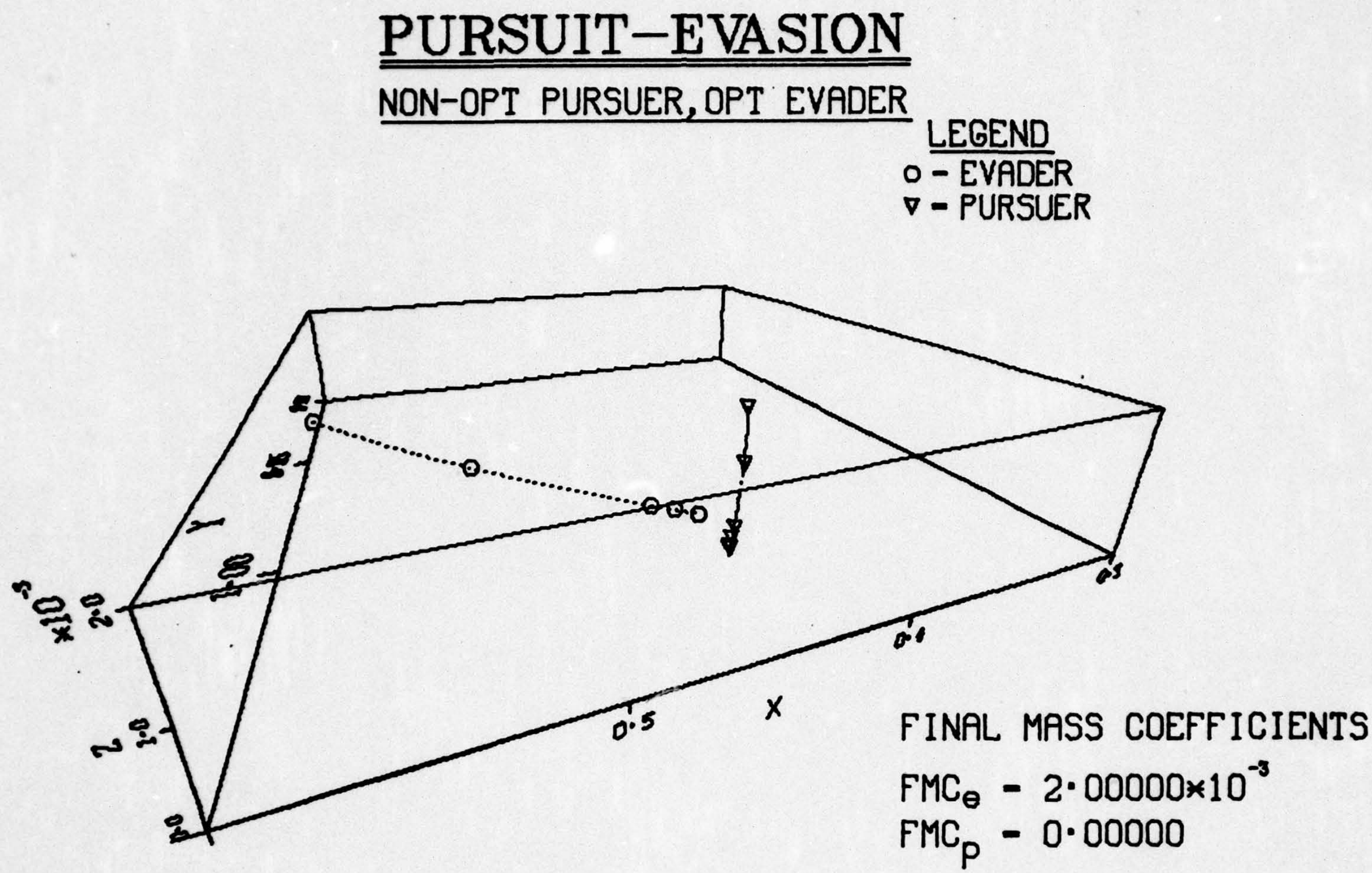

Fig. B-19 Case 3 AK = 1.0 X 10^{-11}

PURSUIT–EVASION

NON-OPT PURSUER, OPT EVADER

LEGEND
o – EVADER
▽ – PURSUER

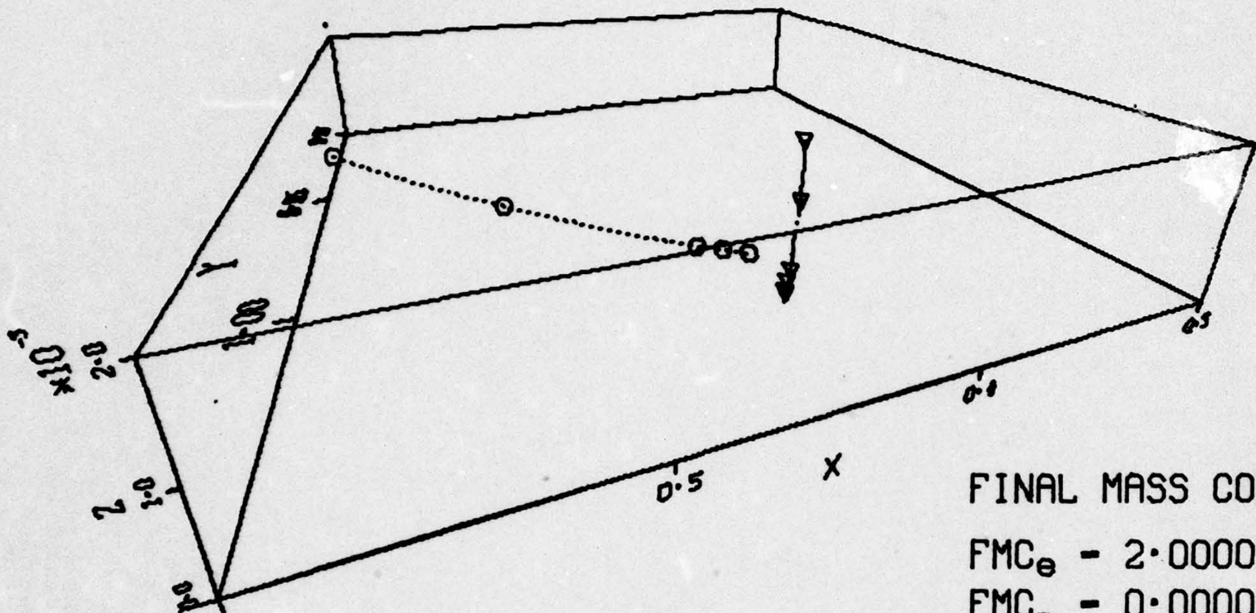

FINAL MASS COEFFICIENTS

FMC_e – $2 \cdot 00000 \times 10^{-3}$

FMC_p – $0 \cdot 00000$

Fig. B-20 Case 3 AK = 10.0×10^{-11}

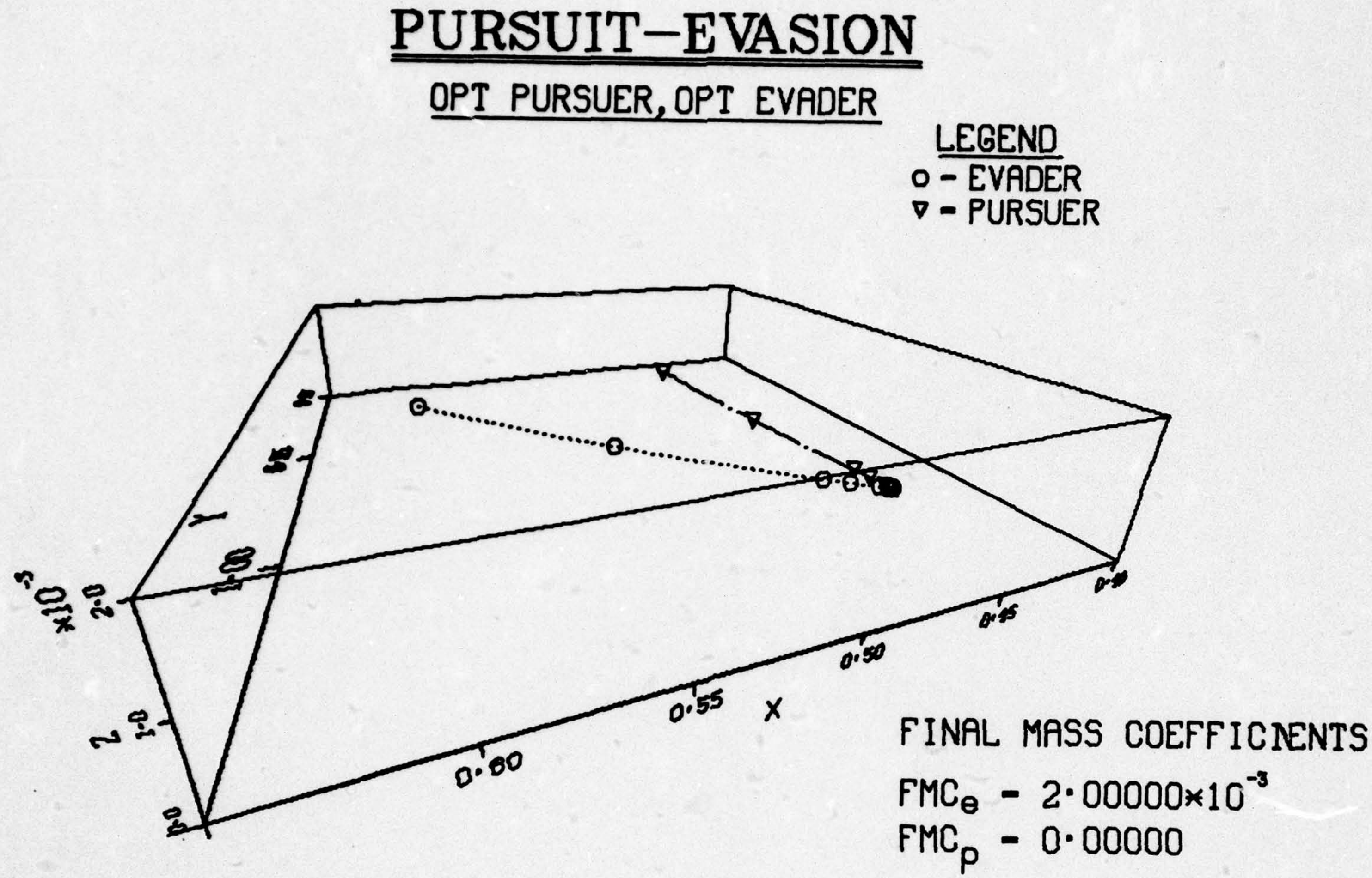

Fig. B-21 Case 4 AK = 0.1 X 10^{-11}

PURSUIT–EVASION

OPT PURSUER, OPT EVADER

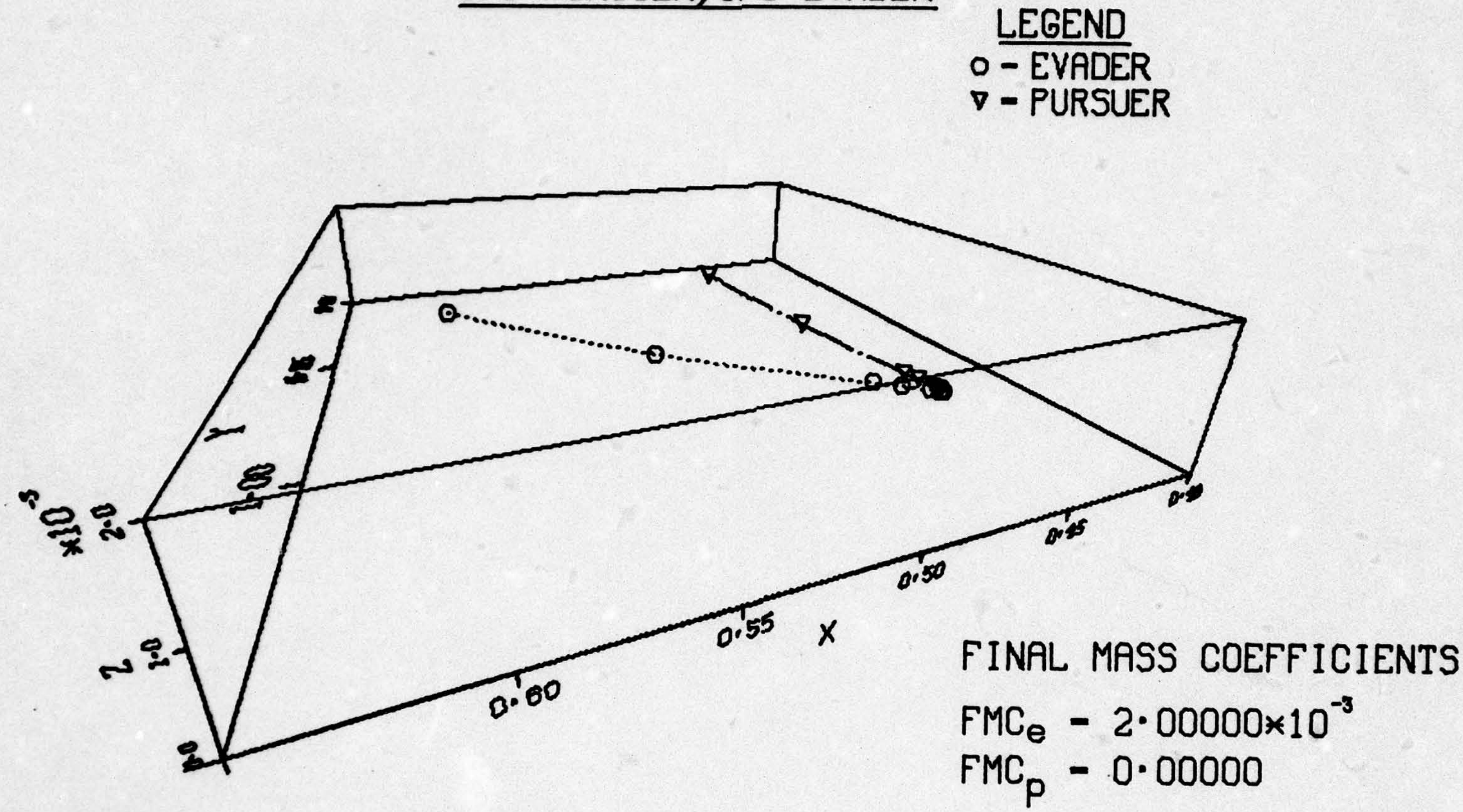

Fig. B-22 Case 4 AK = 1.0×10^{-11}

PURSUIT–EVASION

OPT PURSUER, OPT EVADER

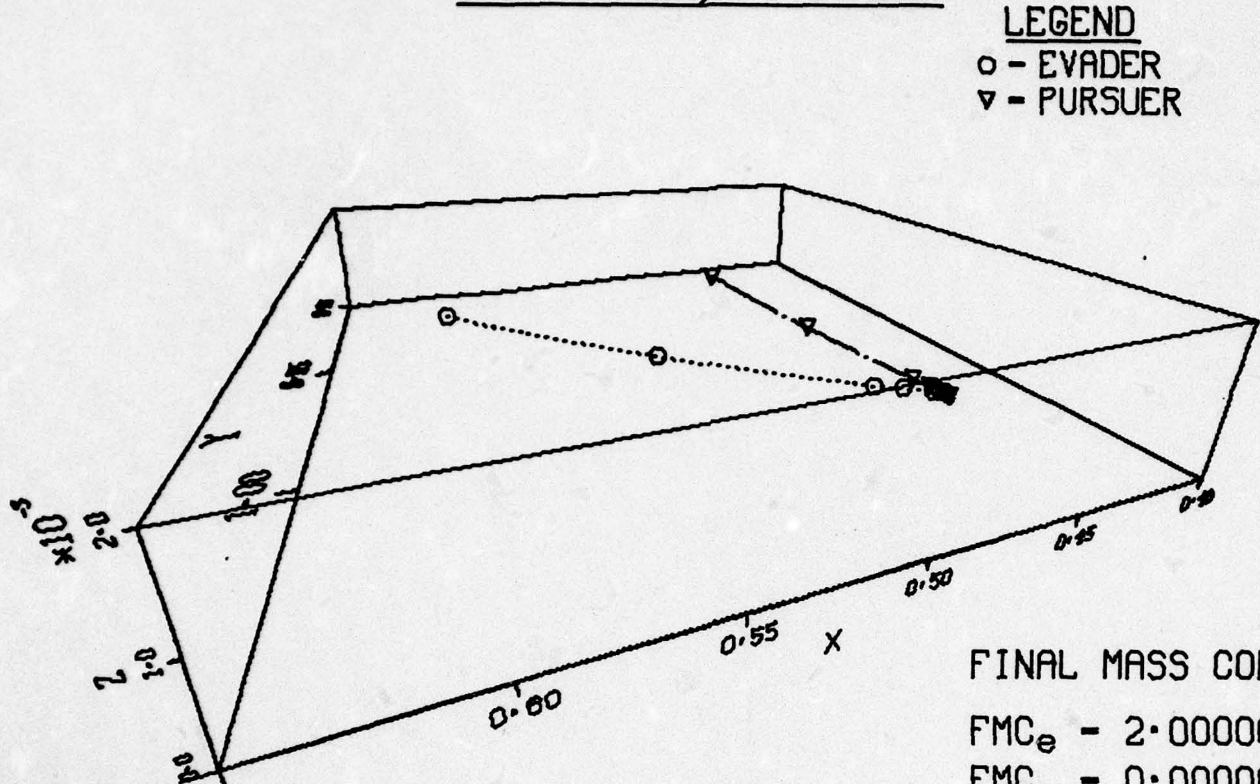

FINAL MASS COEFFICIENTS

FMC_e - $2\cdot00000\times10^{-3}$

FMC_p - $0\cdot00000$

Fig. B-23 Case 4 AK = 10.0×10^{-11}

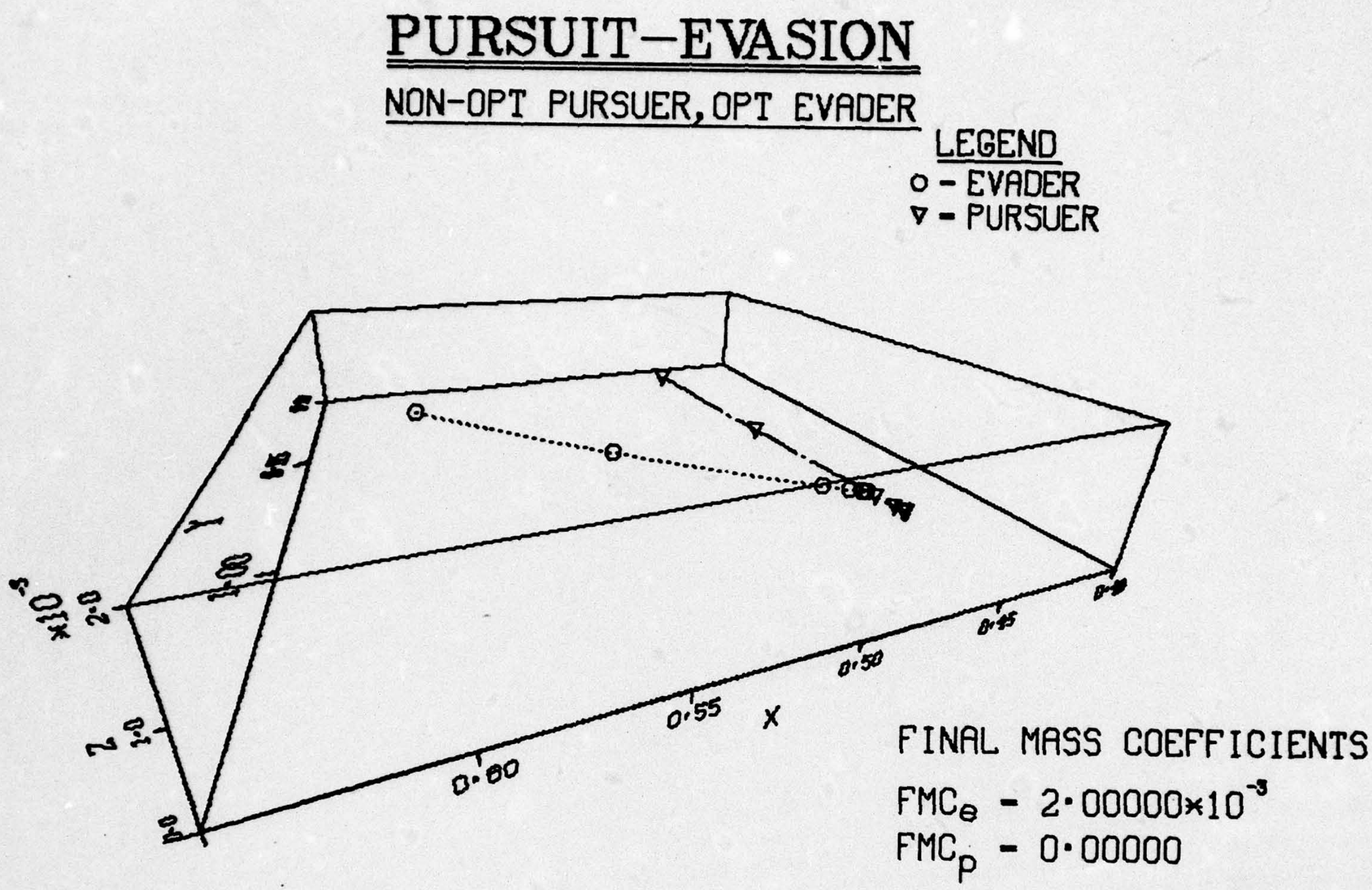

Fig. B-24 Case 4 AK = 0.1 X 10^{-11}

PURSUIT–EVASION

NON-OPT PURSUER, OPT EVADER

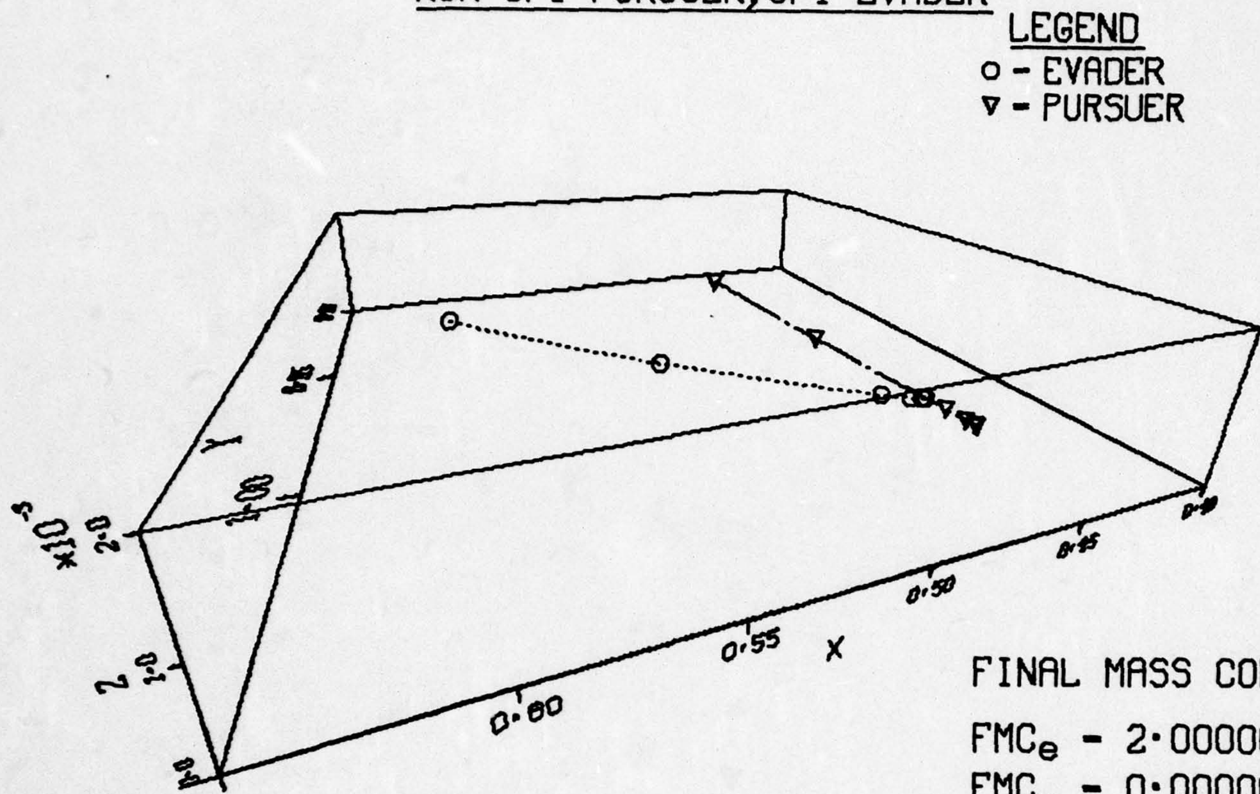

FINAL MASS COEFFICIENTS

FMC_e - 2.00000×10^{-3}

FMC_p - 0.00000

Fig. B-25 Case 4 AK = 1.0×10^{-11}

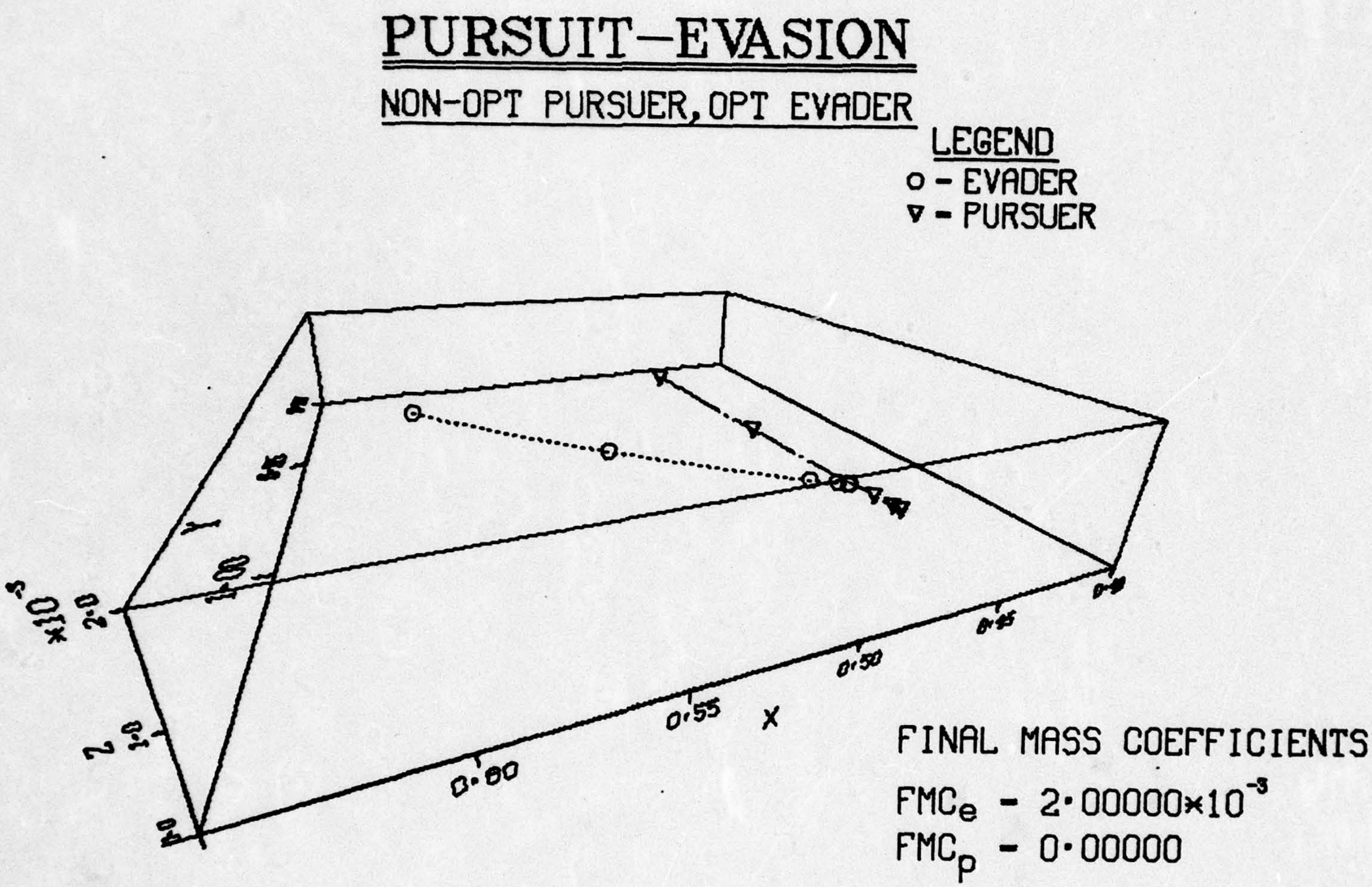

Fig. B-26 Case 4 AK = 10.0 X 10^{-11}

PURSUIT–EVASION

OPT PURSUER, OPT EVADER

LEGEND
o – EVADER
∇ – PURSUER

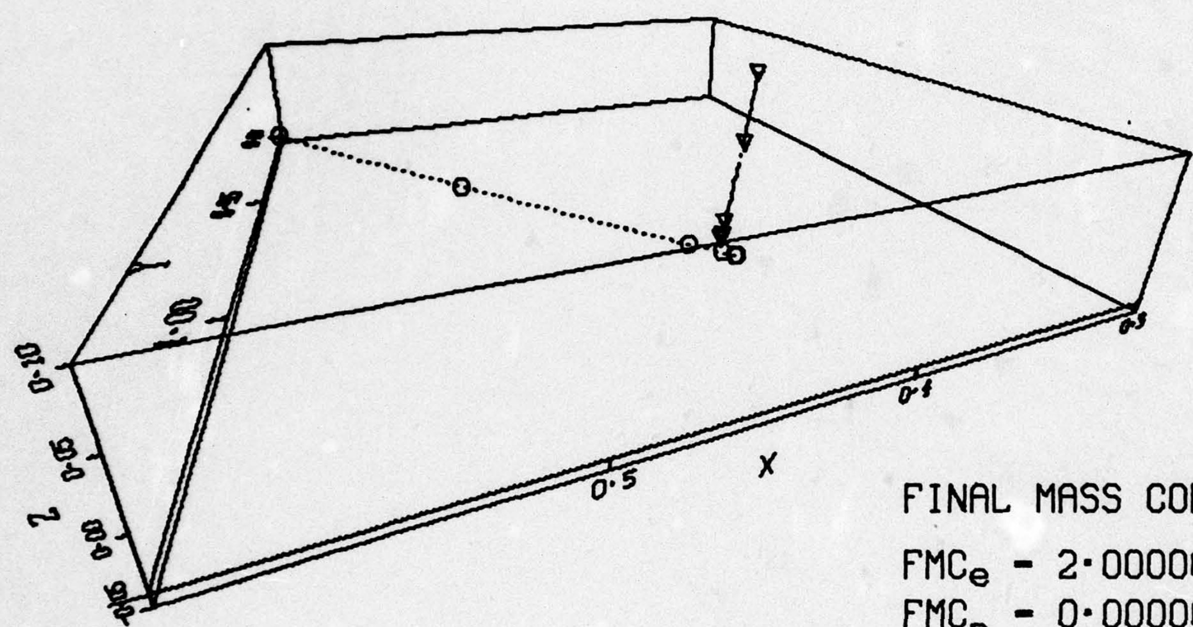

FINAL MASS COEFFICIENTS

FMC_e - $2\cdot00000\times10^{-3}$
FMC_p - $0\cdot00000$

Fig. B-27 Case 5 AK = 0.1×10^{-11}

PURSUIT–EVASION

OPT PURSUER, OPT EVADER

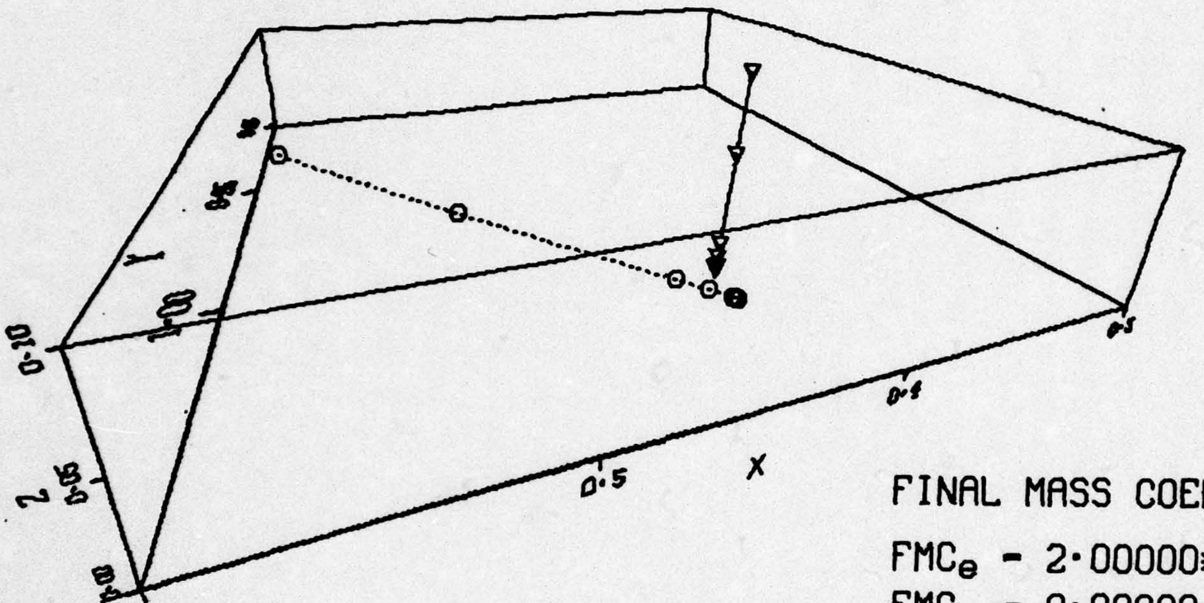

FINAL MASS COEFFICIENTS

FMC_e - 2.00000×10^{-3}

FMC_p - 0.00000

Fig. B-28 Case 5 AK = 1.0×10^{-11}

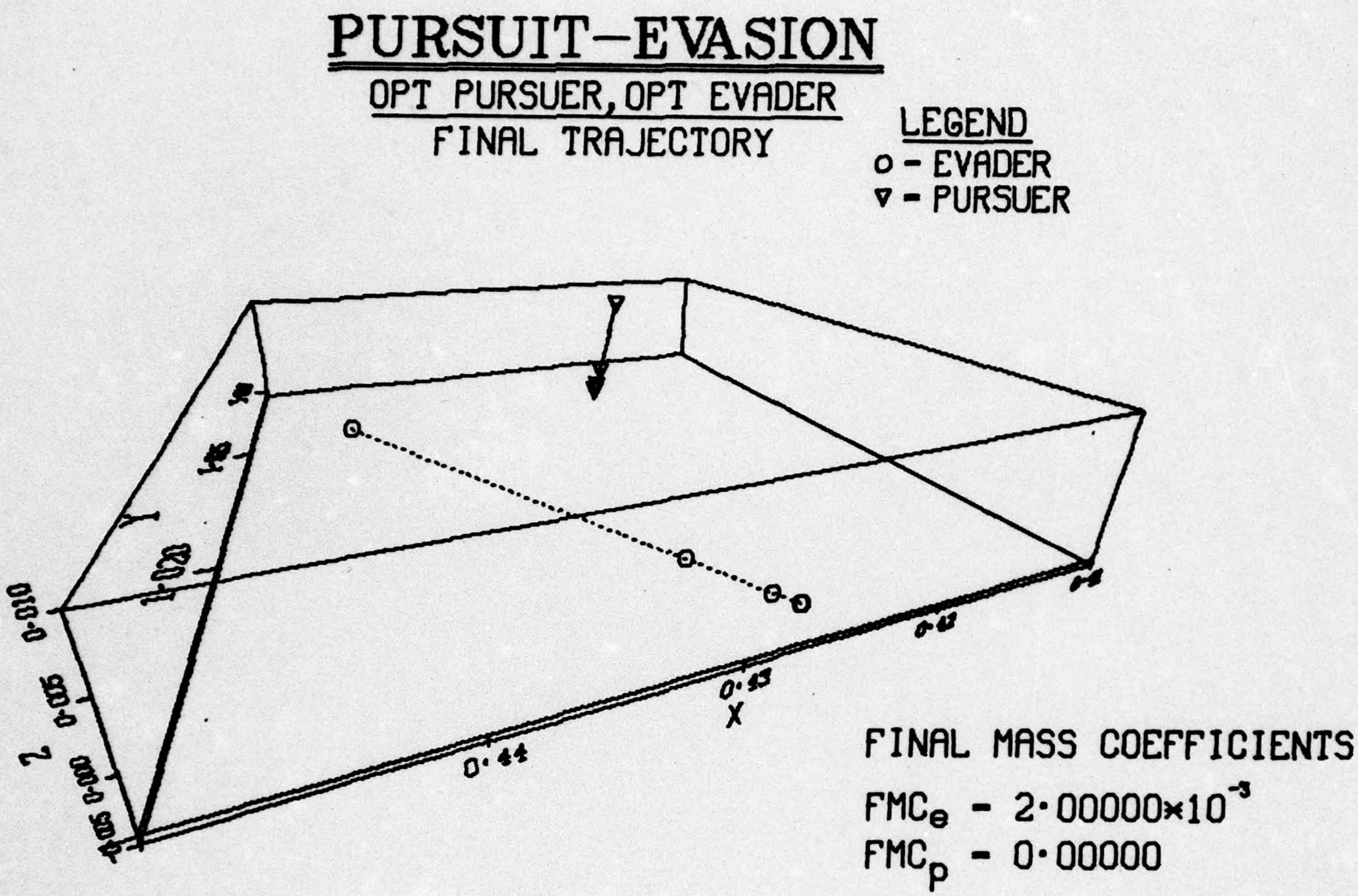

Fig. B-29 Case 5 AK = 1.0 X 10^{-11}

PURSUIT–EVASION

OPT PURSUER, OPT EVADER

LEGEND
o – EVADER
▽ – PURSUER

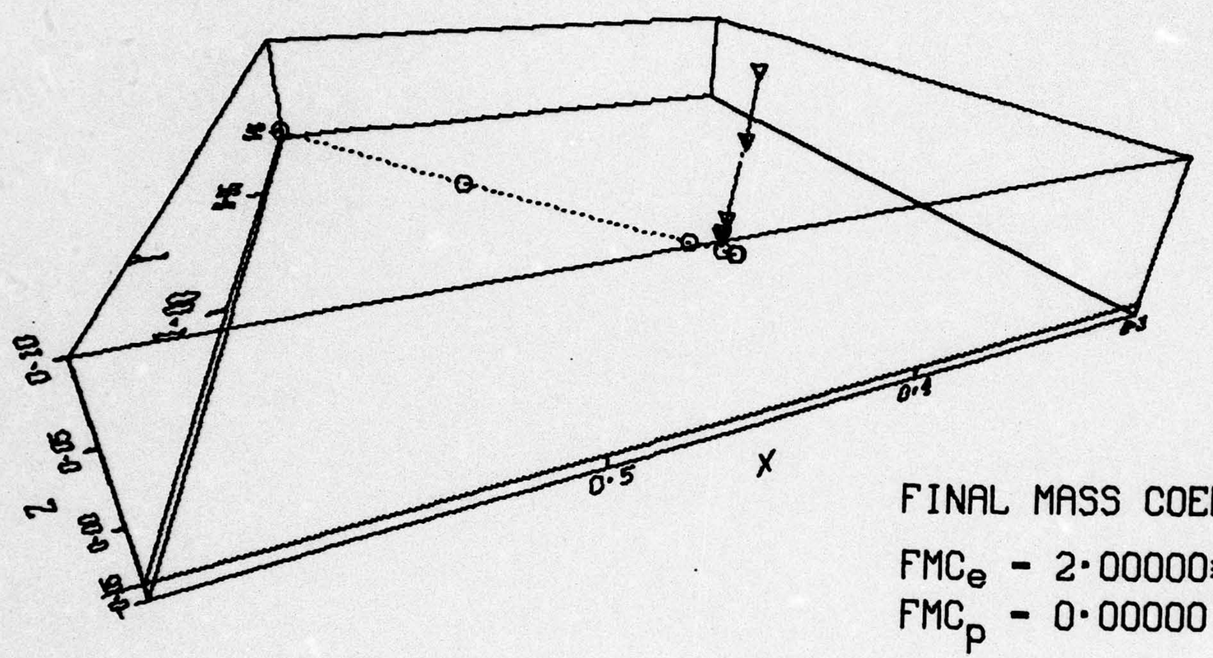

FINAL MASS COEFFICIENTS

FMC_e – $2\cdot00000\times10^{-3}$

FMC_p – $0\cdot00000$

Fig. B-30   Case 5   AK = 10.0×10^{-11}

PURSUIT–EVASION

NON-OPT PURSUER, OPT EVADER

LEGEND
o – EVADER
∇ – PURSUER

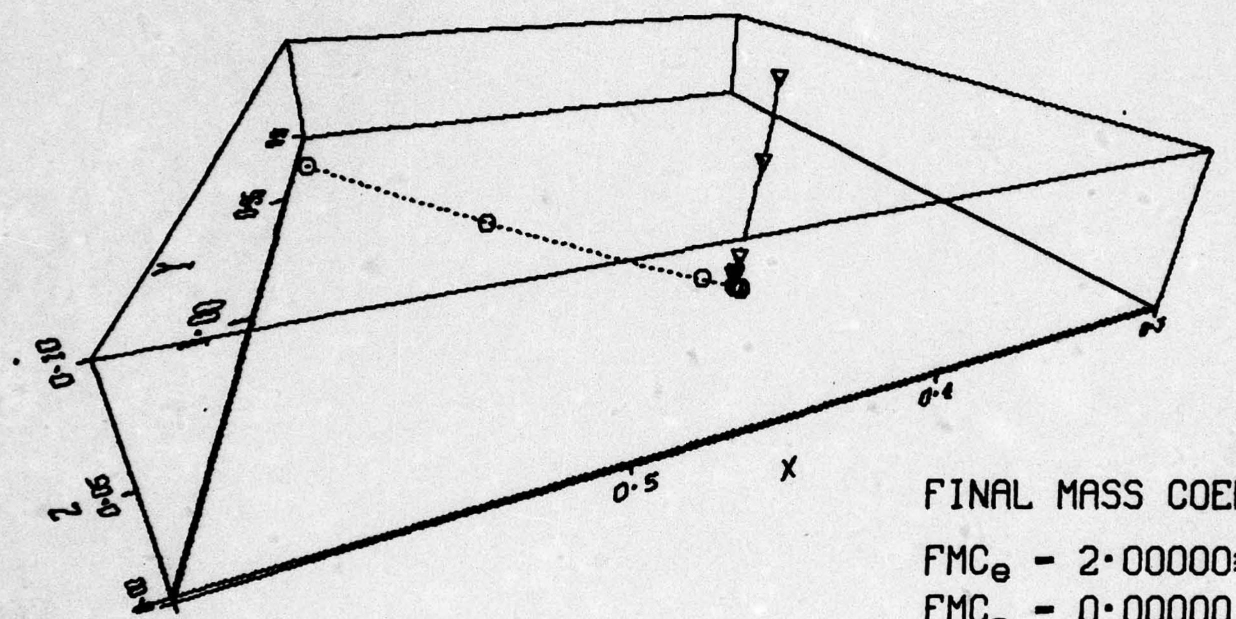

FINAL MASS COEFFICIENTS

FMC_e – $2\cdot00000\times10^{-3}$
FMC_p – $0\cdot00000$

Fig. B-31 Case 5 $AK = 0.1 \times 10^{-11}$

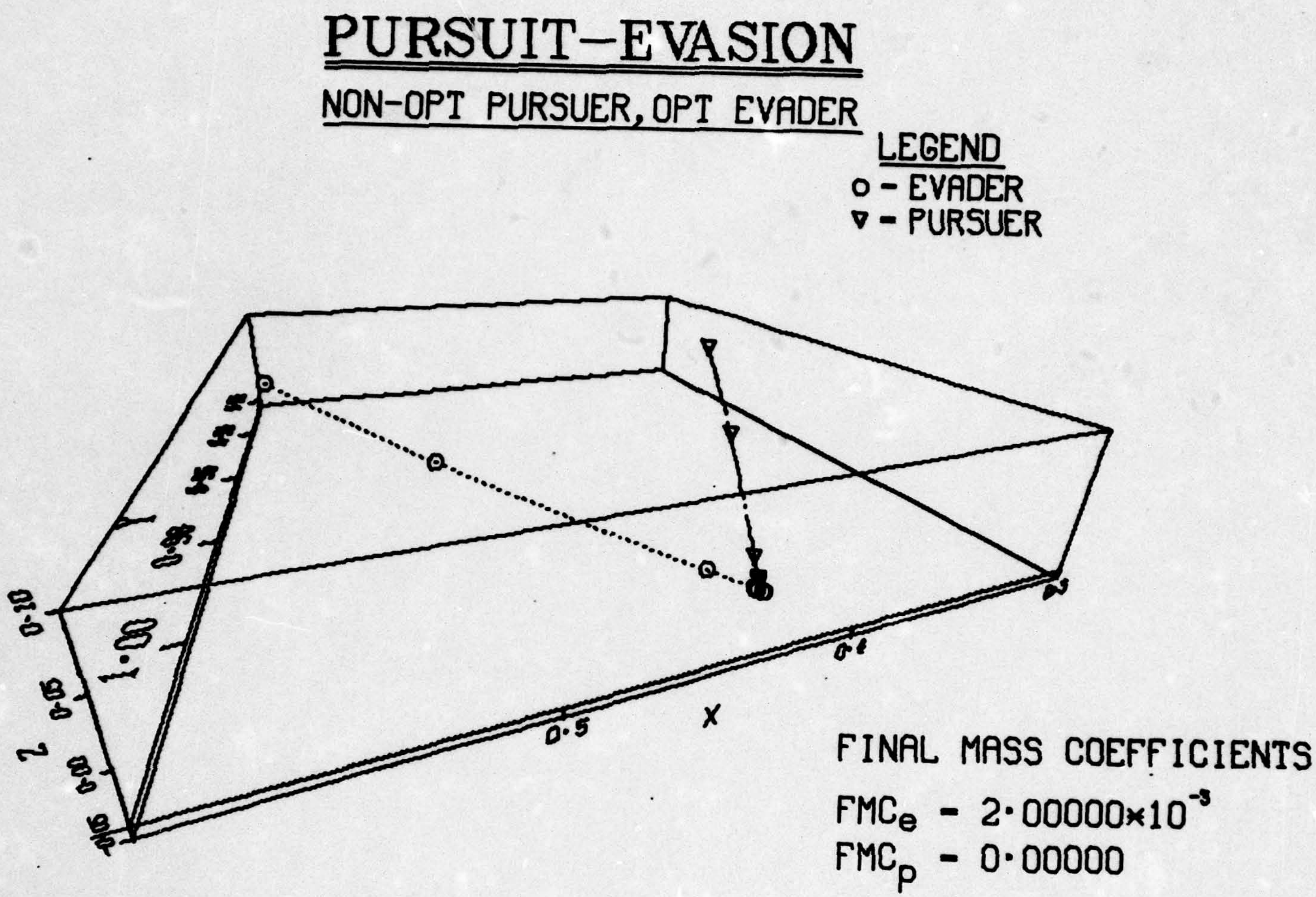

Fig. B-32 Case 5 AK = 1.0 X 10^{-11}

PURSUIT–EVASION

NON-OPT PURSUER, OPT EVADER

FINAL TRAJECTORY

LEGEND

o – EVADER

▽ – PURSUER

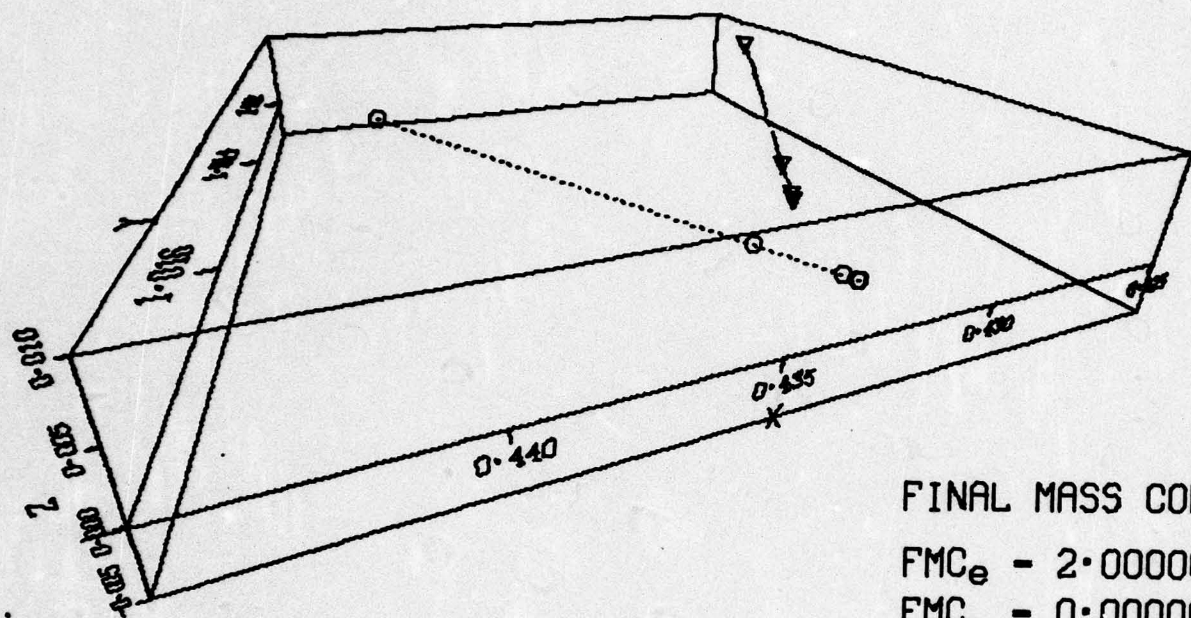

FINAL MASS COEFFICIENTS

FMC_e – $2 \cdot 00000 \times 10^{-3}$

FMC_p – $0 \cdot 00000$

Fig. B-33 Case 5 AK = 1.0×10^{-11}

PURSUIT–EVASION

NON-OPT PURSUER, OPT EVADER

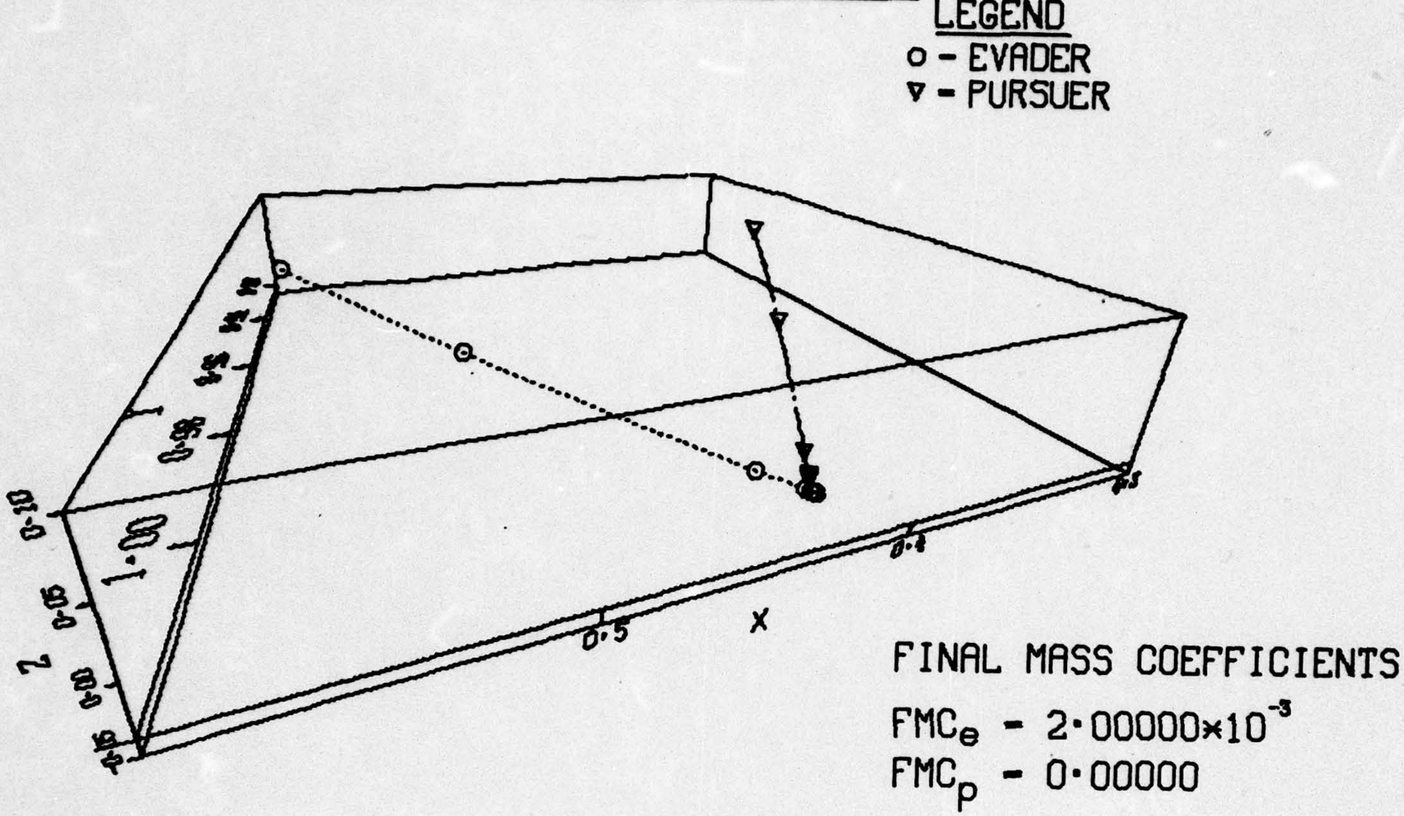

Fig. B-34 Case 5 AK = 10.0×10^{-11}

Vita

William V. Green was born in Morgantown, West Virginia on December 11, 1947. He graduated from high school in Louisville, Kentucky and accepted an appointment to the Air Force Academy. He graduated from the Academy with a degree in Aeronautical Engineering and began pilot training at Vance AFB, Oklahoma. He flew the C-123K in Vietnam. He then flew the T-37 as an instructor pilot, and a member of the Wing Operations staff at Sheppard AFB, Texas. In June 1975, he entered the Air Force Institute of Technology's graduate program in Astronautical Engineering.

UNCLASSIFIED

SECURITY CLASSIFICATION OF THIS PAGE (When Data Entered)

REPORT DOCUMENTATION PAGE		READ INSTRUCTIONS BEFORE COMPLETING FORM
1. REPORT NUMBER GA/MC/76D-8	2. GOVT ACCESSION NO.	3. RECIPIENT'S CATALOG NUMBER
4. TITLE (and Subtitle) A Fuel Conservation Near-Optimal Control Law for an Evading Spacecraft		5. TYPE OF REPORT & PERIOD COVERED MS Thesis 6. PERFORMING ORG. REPORT NUMBER
7. AUTHOR(s) William V. Green Capt. USAF		8. CONTRACT OR GRANT NUMBER(s)
9. PERFORMING ORGANIZATION NAME AND ADDRESS Air Force Institute of Technology (AFIT/EN) Wright Patterson AFB, Oh 45433		10. PROGRAM ELEMENT, PROJECT, TASK AREA & WORK UNIT NUMBERS
11. CONTROLLING OFFICE NAME AND ADDRESS		12. REPORT DATE Dec 1976 13. NUMBER OF PAGES 68
14. MONITORING AGENCY NAME & ADDRESS(if different from Controlling Office)		15. SECURITY CLASS. (of this report) UNCLASSIFIED 15a. DECLASSIFICATION/DOWNGRADING SCHEDULE

16. DISTRIBUTION STATEMENT (of this Report)

Approved for public release; distribution unlimited.

17. DISTRIBUTION STATEMENT (of the abstract entered in Block 20, if different from Report)

18. SUPPLEMENTARY NOTES

Approved for public release
IAW AFR 190-17
Jerral F. Guess, Capt. USAF
Director of Information

19. KEY WORDS (Continue on reverse side if necessary and identify by block number)

Satellite evasion
Differential Game
Optimal control
Fuel optimazation
Pursuit-evasion

20. ABSTRACT (Continue on reverse side if necessary and identify by block number)

A fuel conservation control law for an evading spacecraft is tested in a free final time,pursuit-evasion differential game.
A form of differential dynamic programming with periodic updating is used to solve the optimal control problem. The control law is tested against two different kinds of pursuers. One of the pursuers is using the same updating of the optimal control scheme and the other pursuer is using a non-optimal control law. The non-optimal control law produces a collision course between the two craft. → over

DD FORM 1 JAN 73 1473 EDITION OF 1 NOV 65 IS OBSOLETE

UNCLASSIFIED

SECURITY CLASSIFICATION OF THIS PAGE (When Data Entered)

20. The evader is able to take advantage of any non-optimal play by the pursuer. The evader is able to optimize the combination of fimal range and final mass, depending on the mission.

Plots comparing the flight path of the evader and several different pursuers are included.